Ecological Informatics 87 (2025) 103103

Contents lists available at ScienceDirect

Ecological Informatics

journal homepage: www.elsevier.com/locate/ecolinf

Seasonal and inter-annual dynamics of a *Macrocystis pyrifera* forest in Concepcion Bay, Chile

Daniel Gonzalez-Aragon [a,b,*], Richard Muñoz [c], Henry Houskeeper [d], Kyle Cavanaugh [e], Wirmer García-Tuñon [a,j], Laura Farías [b,f,g], Carlos Lara [h], Bernardo R. Broitman [b,i]

[a] *Doctorado en Ciencias mención en Biodiversidad y Biorecursos, Facultad de Ciencias, Universidad Católica de la Santísima Concepción, Concepción, Chile*
[b] *Instituto Milenio en Socio-Ecología Costera (SECOS), Chile*
[c] *Programa de Doctorado en Oceanografía, Departamento de Oceanografía, Universidad de Concepción, Concepción, Chile*
[d] *Department of Applied Ocean Physics and Engineering, Woods Hole Oceanographic Institution, USA*
[e] *Department of Geography, University of California, Los Angeles, CA, USA*
[f] *Departamento de Oceanografía, Universidad de Concepción, Concepción, Chile*
[g] *Center for Climate and Resilience Research (CR2), Universidad de Chile, Santiago, Chile*
[h] *Departamento de Ecología, Facultad de Ciencias, Universidad Católica de la Santísima Concepción, Concepción, Chile*
[i] *Departamento de Ciencias, Facultad de Artes Liberales, Universidad Adolfo Ibáñez, Viña del Mar, Chile*
[j] *Data Observatory Foundation, ANID Technology Center No. DO210001, Santiago, Chile*

A R T I C L E I N F O

Dataset link: https://code.earthengine.google.com/df92ced1763815d2d520dc23ab0b5814, https://doi.org/10.5281/zenodo.14975329

Keywords:
Remote sensing
Macrocystis pyrifera
Seasonal variation
Chile kelp forest

A B S T R A C T

Kelp forest are foundation species that deliver key ecosystem services for coastal habitats. Chile is one of the largest exporters of kelp biomass, which relies on the harvesting of wild populations. The vast and rugged coastline of Chile hinders field-based studies of the seasonal and spatial dynamics of kelp biomass, yet remote sensing approaches can provide an effective tool to study temporal patterns of kelp distribution and biomass. Our study aimed to establish the basic patterns of variation in the surface area and biomass of a *Macrocystis pyrifera* forest off Concepcion Bay, Central Chile. Using archival data from the Landsat series we constructed a long-term series of annual kelp canopy cover and assessed patterns of interannual, and a seasonal variation with the more recent Sentinel 2 data using Google Earth Engine. We validated satellite observations of the kelp forest in the field by recording local temperature and nutrient concentrations and through a sample of blades and stipes, which we used to estimate whole-individual *in situ* biomass through allometric relationships. Finally, we related decadal to interannual changes in canopy cover to local and regional drivers using data from public repositories. Our 24-year annual time series revealed large year-to-year variability in kelp forest area that did not show a significant association with different El Niño-Southern Oscillation indices, but the deviance explained increased notably with a 1-year lag. The seasonal time series exhibited clear seasonal patterns with cover peaking during summer. We found a significant influence of local environmental variables such as temperature, wave height, nitrate concentration, and solar radiation on kelp forest area. Furthermore, blade counts appeared as the most reliable metric for estimating *M. pyrifera* biomass. Interestingly, we found no evidence of temperature or nutrient stress during the summer biomass peak, hence seasonal variation in *M. pyrifera* abundance appears to be primarily influenced by solar radiation and wave activity in our study population. Our results provide a basis to derive seasonal time series across Chile's kelp forests and suggest that understanding local stressors is key to ensure harvesting practices that promote the sustainable management of these key habitats. As ongoing climate change and overexploitation threaten kelp forest habitats, remote sensing emerges as a promising tool for the monitoring and management of extensive and remote coastlines.

1. Introduction

Coastal kelp forests, together with coral reefs and estuaries, rank among the most productive marine ecosystems in the global ocean (Duarte et al., 2022). They provide key ecosystem services by supplying habitat and food for different fisheries and acting as a fishery resource themselves (Pessarrodona et al., 2022; Eger et al., 2023). Among

* Corresponding author at: Doctorado en Ciencias mención en Biodiversidad y Biorecursos, Facultad de Ciencias, Universidad Católica de la Santísima Concepción, Concepción, Chile.
E-mail address: dgonzalez@doctorado.ucsc.cl (D. Gonzalez-Aragon).

https://doi.org/10.1016/j.ecoinf.2025.103103
Received 30 November 2024; Received in revised form 6 March 2025; Accepted 7 March 2025
Available online 19 March 2025

macroalgae, the order Laminariales—kelps—stand out following their characteristic habitat-forming strategy; mature forests generate complex three-dimensional environments that sustain high rates of primary productivity and harbor complex food webs (Steneck et al., 2002; Reed and Brzezinski, 2009). In the Humboldt Current System, along western South America, the importance of kelp is heightened by the reliance of coastal socio-ecological systems on these forests (Cuba et al., 2022). Chile is one of the largest exporters of wild kelp in the world; all kelp species that occur along the coastline are harvested, particularly over the northern region (Vásquez et al., 2024). There is considerable concern regarding the sustainability of kelp harvesting as overexploitation can have negative impacts on the entire ecosystem given the foundational role played by these forest-forming species (Buschmann et al., 2014; Vásquez, 2016).

Management plans and sustainable exploitation strategies for wild populations should be grounded in a thorough comprehension of their spatial and temporal ecological dynamics, biology, and ecology (Mace and Reynolds, 2001; Betancourtt et al., 2018; Krausman and Cain, 2022). However, monitoring of kelp forests along the Chilean shorelines poses major challenges given the large extent and the steep coastal topography along the main kelp harvesting areas (Frangoudes et al., 2011; Vásquez, 2016). While some studies have explored the distribution and abundance of exploited kelp species along the Humboldt Current, large-scale analyses remain limited (Carranza et al., 2024). Most surveys have focused on local populations and used disparate methodologies that hinder comparison of changes in kelp forest area or biomass over time (Vásquez, 2016). In this context, the study of the dynamics of kelp populations along the Chilean coast requires the adoption of innovative approaches, such as remote sensing with satellite images. Remote sensing has been used to observe the area, biomass, and distribution of macroalgae and seagrasses with high accuracy (Fornes et al., 2006; Setyawidati et al., 2018; Mora-Soto et al., 2020), and has been shown to be more time- and cost-effective than *in situ* sampling (Cavanaugh et al., 2010, 2011; Nijland et al., 2019; Bell et al., 2020; Hamilton et al., 2020). Remote sensing methods are powerful tools for mapping kelp forests; however, they are not without limitations that can affect the accuracy of the results. Tidal fluctuations, for instance, can influence the visibility and extent of the canopy at the sea surface, leading to false positives or false negatives in detection (Cavanaugh et al., 2011; Bell et al., 2015a). Variations in water turbidity, atmospheric conditions, and satellite sensor resolution further contribute to uncertainties in estimating kelp forest distribution and biomass (Cavanaugh et al., 2021a; Timmer et al., 2024). These challenges are compounded by the logistical difficulty of acquiring sufficient training and validation data in remote locations, which can result in underestimations of prediction errors and reduced robustness of remote sensing models (Mora-Soto et al., 2020, 2022). Addressing these limitations is essential to improving the reliability of remote sensing-based assessments of kelp forest ecosystems. Failure to account for these constraints risks inaccuracies that could undermine effective management and conservation efforts (Bennion et al., 2019). By integrating field-based studies with remote sensing tools, we can advance our understanding of the functioning and regulation of large coastal ecosystems, paving the way for more informed and effective ecosystem management strategies.

Kelp forest mapping research has primarily focused on the estimation of the floating canopy area, which can represent approximately 90% of the total biomass (Reed et al., 2015a). Less attention has been given to biomass estimation of whole kelp forests, as they necessitate the development of specific relationships between *in situ* floating canopy measurements and satellite imagery (McPherson and Kudela, 2022). California Current is at the forefront with its long-term monitoring program of the Santa Barbara region by the Santa Barbara Coastal LTER, which has enabled the use of allometric calculations to estimate biomass from kelp morphological measurements (Rassweiler et al., 2018; Santa Barbara Coastal et al., 2021). Time series of canopy biomass have been derived from these data in conjunction with Landsat satellite images (Cavanaugh et al., 2011; Bell et al., 2015a). However, the lack of data in other regions limits extrapolations of biomass estimations and, consequently, large-scale estimates of carbon sequestration and primary productivity rates from satellite data (McPherson and Kudela, 2022). For example, it is unclear the degree to which kelp length-to-weight relationships vary regionally. Recently, a step forward was made at the Chilean sub-Antarctic ecoregion with a estimation of net primary production on three natural populations, enhancing our understanding of sub-Antarctic kelp's role in carbon flux (Palacios et al., 2024). With Chile's extensive coastline hosting a variety of kelp species, developing specific local and species biomass relationships is essential for the future management of these marine forests.

The giant kelp, *Macrocystis pyrifera* C. Agardh (1820), is widely distributed along temperate shores worldwide (Graham et al., 2007). A number of studies in populations of *M. pyrifera* along the coast of southern Australia, Chile and California have shown that the growth of subtidal stands are strongly seasonal and depend on the supply of nutrients by different oceanographic processes, together with low-frequency, large-scale climatic disturbances such as El Niño-Southern Oscillation (ENSO) cycles (Dayton et al., 1999; Reed et al., 2011). Temperature plays a crucial role on *Macrocystis* life cycle, varying according to the local adaptation of populations to different latitudes (Schiel and Foster, 2015; Hollarsmith et al., 2020). Nitrogen has been identified as a key nutrient showing variations with blade age (Rodriguez et al., 2016), correlations with growth rates within the kelp forest (Stewart et al., 2009), and uptake efficiency dependent on nutrient concentration during growth (Kopczak et al., 1991). Along the coast of Chile, local *M. pyrifera* populations show different responses to stressors, including shifts in their dynamics and reproductive strategies under varying wave exposures (Buschmann et al., 2006), or alterations in reproductive success amid climate change (Hollarsmith et al., 2020).

The exploitation of *M. pyrifera* in Chile has been on the rise, averaging 26,498 tons per year between 2008 and 2020, resulting in a cumulative extraction of 344,472 tons (SERNAPESCA, 2021). The Atacama coast, in northern Chile is the primary hub for the harvest of giant kelp, which is scarcely monitored and has recently been linked to fluctuations in the copper industry (Vásquez, 2016; SERNAPESCA, 2021; Vásquez et al., 2024). Distribution models projected under consensus climate change scenarios for the future forecast a loss of habitat suitability for *M. pyrifera* along the coast of northern Chile (Gonzalez-Aragon et al., 2024; Assis et al., 2023). At the other extreme, the western shores of Patagonia along southern Chile host giant kelp forests that are not yet exploited; two centuries of records document their resilience and identify the zone as a climatic refuge (Friedlander et al., 2018; Huovinen et al., 2020; Mora-Soto et al., 2021). Along central Chile, *M. pyrifera* extraction is also minimal (SERNAPESCA, 2021). Light and nutrient levels can be consistently high throughout the year, enabling continuously high *M. pyrifera* sporophyte productivity (Graham et al., 2007).

The ecological and economic importance of wild giant kelp populations in Chile, coupled to the extensive range of environmental conditions found along the vast coastline reinforces the importance of understanding temporal patterns of spatial variability and the identify the drivers of kelp abundance dynamics. Hence, monitoring over long time scales is a key knowledge gap that we may partially fill using remote sensing, which can be supplemented through targeted field sampling to understand the role of local environmental and ecological processes (Cavanaugh et al., 2021a; Carranza et al., 2024). Our study aimed to establish basic patterns of variation in surface cover of a *M. pyrifera* forest off Central Chile and pinpoint its key drivers using data collected in the field, from public repositories and remote sensing. As an initial step, we analyze interannual to decadal variations in the resultant kelp area time series to evaluate the potential influence of climatic factors, including ENSO and sea surface temperature changes. Subsequently, we examine variables affecting the retrieval of giant

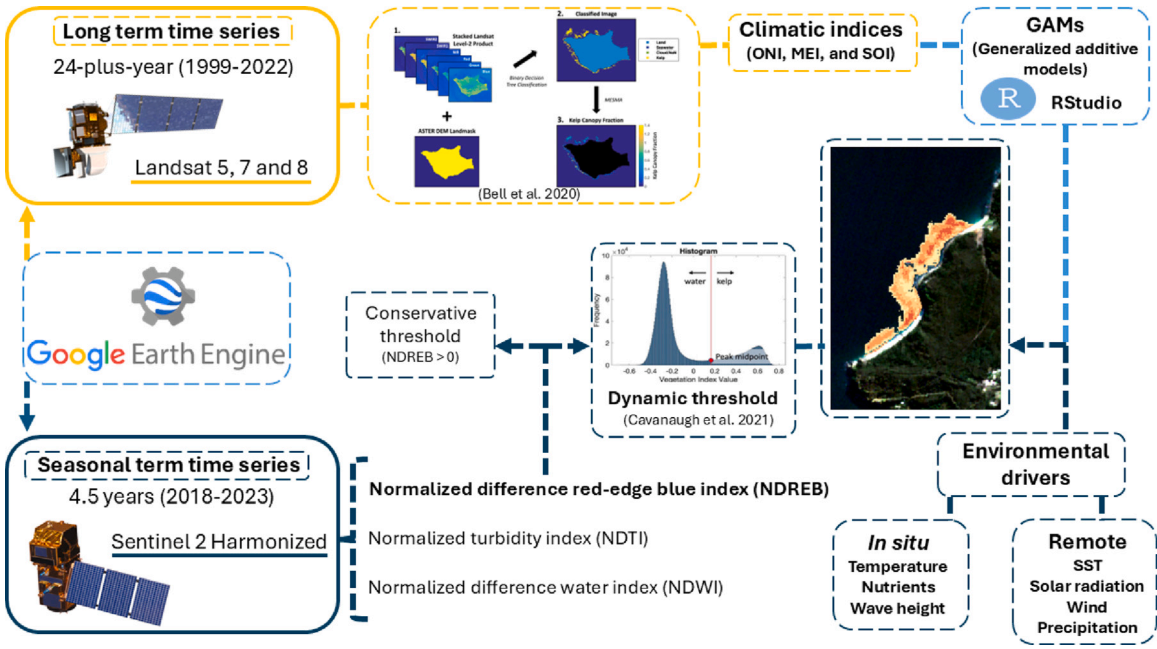

Fig. 1. Methodological workflow diagram. The workflow begins with Google Earth Engine, branching into two main paths. At the top (yellow), the process involves using Landsat data to create a long-term time series following the methodology described by Bell et al. (2020). This culminates in GAM analyses linking the time series with climate indices. The bottom and center (dark blue) represent the creation of a seasonal time series using Sentinel-2. The workflow starts by applying various water, turbidity, and vegetation indices. From the vegetation index, we derive the seasonal time series, applying and comparing two thresholds, ultimately selecting the dynamic threshold. Finally, this time series was analyzed using GAMs against various in situ and remote environmental variables. (For interpretation of the references to color in this figure legend, the reader is referred to the web version of this article.)

kelp forest surface cover using remote sensing. Additionally, we aim to understand seasonal changes in area in relation to environmental factors measures in the field such as local ocean temperature and nutrient availability, and from public repositories such as wave height, wind and solar radiation. Finally, we present an approximation of local biomass estimation derived from our direct measurements and satellite imagery. Remote sensing may thus comprise a highly valuable methodology for the extensive and remote Chilean coast, and could emerge as an approach for conservation.

2. Methods

A schematic representation of the methodological workflow is provided in (Fig. 1). The components of this workflow are further elaborated upon in the subsequent sections. In this study, we used data from two different satellite platforms (Landsat and Sentinel-2; Table 5).

2.1. Study area

Our study was conducted on a population of *M. pyrifera* occupying the shoreline off Punta de Parra, situated at the northeastern side of Concepción Bay (CB)(Fig. 2). The CB has a nearly rectangular shape and it opens to the ocean on the north-facing side (Sobarzo et al., 1997). It is a shallow semi-enclosed system spanning 190 km^2 of surface area with maximum width of 12.5 km and a maximum depth of 48 m (Sobarzo et al., 1997). The bay receives a fluvial contribution from river and nearby estuaries together with several point-sources from industrial and urban activity (Ramón et al., 1983; Silva et al., 1987; Rudolph et al., 2002). Two contrasting wind regimes characterize CB: southwest winds dominate from September to March, and north winds prevail from May to July (Saavedra, 1980). The transfer of wind momentum over the sea surface within CB leads to the formation of two layers exhibiting nearly anti-parallel directions (Sobarzo et al., 1997). Winds blowing from the north drive surface water into the bay, resulting in a compensating outflow near the bottom. Conversely, south winds drive surface water circulation outward and the infiltration of a bottom layer of water. Coastal upwelling is strongly seasonal and peaks during spring and summer months when the equatorward winds intensify and temperatures drop below 14°C, indicative of recently upwelled water (Sobarzo et al., 2007; Farías et al., 2021). Seasonal coastal upwelling is the primary driver of productivity and drives seasonal variation within CB (Sobarzo et al., 2007). Sediments plays a pivotal role as a nutrient source rather than a sink, with organic nitrogen remineralization reaching percentages of 73%–86% via benthic regeneration (Farias et al., 1996). Recently, alterations in this regime were attributed to the increased upwelling strength following an intensification of the South Pacific Anticyclone, even during winter, along with shifts in precipitation patterns (Schneider et al., 2017; Farías et al., 2021; Bustos-Espinoza et al., 2024).

2.2. Long term annual canopy series with Landsat dataset

To reconstruct interannual changes in the forest area of *M. pyrifera* at Punta de Parra, we developed a time series of emergent kelp forest canopy following Cavanaugh et al. (2010) and using imagery from the Landsat 5 (L5) Thematic Mapper (TM), Landsat 7 (L7) Enhanced Thematic Mapper Plus (ETM+), and Landsat 8 (L8) Operational Land Imager (OLI) satellites. Although the satellites leveraged included observations beginning in approximately 1984, valid images for our study domain were available from 1999 to 2022. Recently, the advent of cloud-based platforms like Google Earth Engine (GEE) has streamlined the process of working with satellite images, significantly reducing the time required for large-scale geoprocessing and analysis (Gorelick et al., 2017). The Application Programming Interface (API) of GEE enables real-time visualization of outcomes, and the availability of open-access satellite imagery datasets expedites longitudinal population monitoring (Pérez-Cutillas et al., 2023). Landsat Collection 1 Level-2 reflectance data were accessed and processed via GEE to develop a 24-plus-year time series of emergent kelp forest canopy. The pixel classification was performed using a two-step process, in which: (1) a decision tree classifier identified likely kelp containing pixels; and (2) kelp coverage within each pixel was assessed using

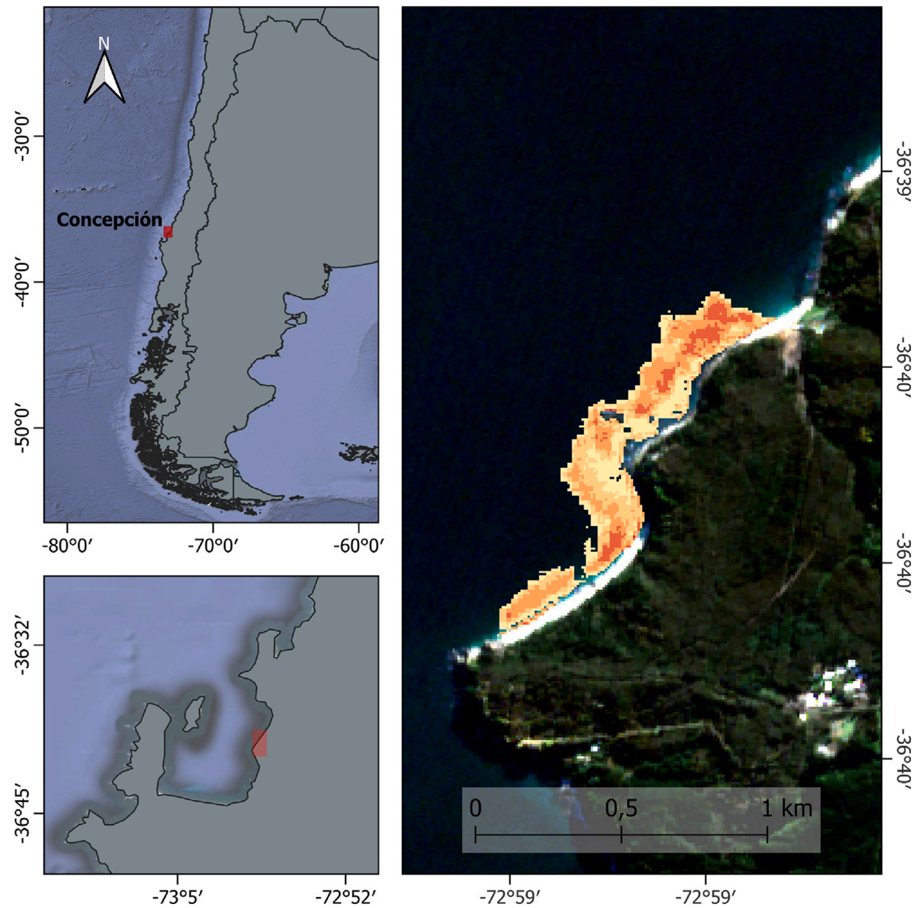

Fig. 2. Population of *Macrocystis pyrifera* at Punta de Parra, Concepción, Chile. The top left panel shows a map of South America, with the study area highlighted in a red box. The bottom left panel provides a closer view of Concepción Bay, with Punta de Parra highlighted in another red box. On the right, the Sentinel-2 Harmonized Level 2A image is displayed in RGB, overlaid with the *M. pyrifera* population delineated using the NDREB index from January 18, 2023. The color gradient represents vegetation index values, with darker red hues indicating the highest values.

Multiple End-Member Spectral unMixing Analysis (MESMA). MESMA served as quality control for the decision tree classifications (pixel values indicating less than 13% coverage were discarded as likely glint; pixel values greater than 300% were discarded as likely rock). All image analyses were performed via GEE. Validation has been performed in the Falkland-Malvinas Islands (Houskeeper et al., 2022), together with image review opportunities by local experts as part of the KelpWatch data pipeline (Bell et al., 2020). We define the annual window using July 1 to June 30 corresponding to the southern hemisphere winter-to-winter cycle centered on the southern hemisphere summer. We compiled one scene per year for the period 1999–2022, representing the mean annual values for each year. Cloudy pixels were masked and excluded from the analysis, resulting in these areas being represented as NaN values in the dataset. To mitigate data loss caused by cloud cover, the analysis leveraged on the high frequency of repeated observations within each year, providing multiple opportunities to retrieve cloud-free pixels in the time series. The approach is less effective in the earlier part of the time series because of the limited number of satellites in orbit. However, with the advent of multiple Landsat generations operating simultaneously in recent decades, the ability to mitigate data loss from cloud cover has significantly improved. The pixel values of the study area were then extracted to calculate the kelp canopy fraction using QGIS v3.22 (QGIS Development Team, 2022). Pearson's correlation was employed to assess the potential relationships between the pixel values of the different sensors: Landsat 5, Landsat 7, and Landsat 8 (R Core Team, 2022).

To evaluate the influence of large-scale climatic disturbances on kelp cover we downloaded monthly data for the Ocean Oscillation Index (ONI), Multivariate ENSO Index (MEI), and Southern Oscillation Index (SOI) data from NOAA (National Oceanic and Atmospheric Administration, 2023). To assess the impact of ENSO indices (ONI, MEI, and SOI) on the long term annual canopy series with Landsat imagery, we employed GAMs (Generalized additive models) analysis with the mgcv (v1.9-1) package to analyze the nonlinear effects of variables in the time series (Wood, 2017; Pedersen et al., 2019; R Core Team, 2022). GAM analysis was performed with a smoothing parameter (k) of 20 for each variable. The analysis utilized a Gaussian family basis "cr" (cubic regression) and the "REML" (restricted maximum likelihood) method. As large-scale climatic oscillations develop over long temporal scales, their effects on *M. pyrifera* populations may be observed with a lag in time. Therefore, we compared the kelp time series with the climatic indices using a 1-year lag to account for potential delayed impacts (Beas-Luna et al., 2020). The GAM analysis was performed using data from the Landsat 7 ETM+ time series, chosen to provide the longest temporal span (2000–2022).

2.3. Seasonal canopy series with Sentinel 2

We extracted Sentinel 2 (S2) Harmonized Level 2A imagery using GEE (Gorelick et al., 2017; Claverie et al., 2018). We chose S2 imagery to observe the seasonality of macroalgae cover because of its temporal and spatial resolution compared to other satellites such as Landsat. This is possible thanks to the constellation of its two identical satellites (S2A/S2B), which are 180° out of phase and achieve a revisit frequency of 5 days at equatorial latitudes. In addition, the Multispectral Instrument (MSI) sensor on board both satellites covers a wider spectral range (ESA, 2015). The shorter revisit time of S2 allowed us to generate a more complete time series over time. In addition, the spatial resolution of S2 is well suited for our coastal population, as it is less susceptible to the influence of reflectance values from rocks, sand, waves and others. To effectively monitor the giant kelp canopies, we initially employed a cloud detection model integrated with a support vector machine (SVM) and cloud-score algorithm detailed in Li et al. (2022). The method is known for its superior accuracy relative to alternative cloud detection approaches (e.g., QA60 band method) and we created a mask around the *M. pyrifera* population for its implementation.

A total of 320 cloud-free scenes were extracted from the study area from imagery collected between December 2018 and June 2023. The normalized difference water index (NDWI) was used to observe the possible effect of sun glint, a direct specular reflection of solar radiation that can affect the visualization of the giant kelp population (1) (Xu, 2006; Fell, 2022). In order to visualize each scene effectively, the NDWI index was incorporated into GEE, as it provides high values in water pixels impacted by sunglint (Fell, 2022). Water turbidity and tidal height are determinant factors that affect the visualization of the giant kelp canopies (Cavanaugh et al., 2021a). We used normalized difference turbidity index (NDTI) as a proxy for water turbidity (2) (Elhag et al., 2019). The NDTI index indicates higher turbidity of water pixels at higher values (close to 0) and lower turbidity of water pixels at more negative values (close to −1) (Lizcano-Sandoval et al., 2022). The NDTI was calculated for the 320 scenes by creating a specific mask around the *M. pyrifera* population so pixels with giant kelp canopy will not influence the reflectance values of water pixels. The mask layer was manually crafted in QGIS v3.22 (QGIS Development Team, 2022), and then imported the shapefile into GEE. Subsequently, the code specified that the scene would be intersected with the mask layer and computed the NDTI. The average of all pixels values would be calculated, and ultimately, the direct output of the average NDTI value was directly visible on the console of the GEE code editor. The height of the tide has an effect on the amount of canopy that is visible at the time of the satellite image acquisition (Bell et al., 2020). To measure the effect of tidal height, data were extracted from Sea level station monitoring facility of the Talcahuano station, depending on which satellite had obtained the scene in our study area (S2A at 14:37 h and S2B at 14:47 h) (ESA, 2015; Flanders Marine Institute (VLIZ); Intergovernmental Oceanographic Commission (IOC), 2023). We used Pearson's correlation to observe the potential association between turbidity and tidal height variables and their influence in visualization.

To quantify *M. pyrifera* forest area, we employed the normalized difference red-edge blue index (NDREB) in GEE (3). Cavanaugh et al. (2021b) compared twenty multispectral vegetation indices and determined that NDREB was the most robust to accurately separate kelp from water pixels under different environmental conditions. The NDREB index outperformed other indices by leveraging on the unique spectral properties of *M. pyrifera*, which is characterized by its high red-edge and low blue reflectance, in contrast to the higher blue and lower red-edge reflectance of water (Cavanaugh et al., 2021b). As a brown alga lacking chlorophyll b, *M. pyrifera* exhibits distinct spectral features compared to green vegetation and algae, including elevated reflectance between the absorption peaks of chlorophyll a and c (Colombo-Pallotta et al., 2006). Combined with seawater's strong blue reflectance, these properties enhance the contrast between the blue and red-edge/NIR regions, making NDREB a highly effective index for detecting brown algae (Bell et al., 2015b; Cavanaugh et al., 2021b).

The indices were calculated based on the S2 bands (see Table 6).

$$\mathrm{NDWI} = \frac{\mathrm{Green}_{B3} - \mathrm{Near\ Infrared\ (NIR)}_{B8}}{\mathrm{Green}_{B3} + \mathrm{Near\ Infrared\ (NIR)}_{B8}} \tag{1}$$

$$\mathrm{NDTI} = \frac{\mathrm{Red}_{B4} - \mathrm{Green}_{B3}}{\mathrm{Red}_{B4} + \mathrm{Green}_{B3}} \tag{2}$$

$$\mathrm{NDREB} = \frac{\mathrm{Red\ edge}_{B5} - \mathrm{Blue}_{B2}}{\mathrm{Red\ edge}_{B5} + \mathrm{Blue}_{B2}} \tag{3}$$

Considering the close proximity of the Punta de Parra kelp bed to the shoreline (Fig. 2), we manually created a mask to minimize the effects of rock, sand, and breaking waves. The buffer facilitated pixel extraction pixel for both the population and the surrounding water. To extract the area of *M. pyrifera* from the scenes we took two approaches: a conservative threshold and a dynamic threshold. The conservative threshold classified the kelp canopy as all pixels with NDREB values > 0, while the dynamic threshold, proposed by Cavanaugh et al. (2021b), provided a novel and adaptable method. To evaluate its performance, particularly under varying conditions such as tides and turbid waters, we included the conservative threshold as a comparison. The dynamic threshold involves an empirical histogram with all pixel values for each scene, which were extracted using GEE. Then, using the findpeaks function from the pracma package of RStudio (Borchers, 2023; R Core Team, 2022), we identified both the water and kelp peaks and defined a peak midpoint as the value between these two peaks. Pixels with a value above the peak midpoint were considered to be kelp canopy. After confirming normality with a Shapiro–Wilk test for the two time series generated using the dynamic and conservative thresholds, we employed Pearson's correlation to examine their linear association (Sedgwick, 2012). We then used multiple linear regression analysis to observe the combined effects of turbidity and sea level on the area of *M. pyrifera* for both the conservative and dynamic thresholds (Faraw, 2015). The area of each scene and the statistical analysis were carried out in RStudio version 2023.9.1.494 (R Core Team, 2022).

2.4. Environmental drivers

To measure the effect of environmental variables on giant kelp forest area, we sampled directly the Punta de Parra population. We chose three sites along the *M. pyrifera* bed: one in the northern, outermost zone of the population, a second in the middle, and a third in the southernmost edge (Fig. 2). We deployed HOBO sensors at approximately 2 meters depth at the three sites to measure the *in situ* temperature every 15 min from December 2021 to January 2023. We determined the average temperature across the three sites and derived the daily average. Sea Surface Temperature (SST) and the anomalies were acquired from NOAA CDR OISST v02r01 (Optimum Interpolation) dataset via GEE for the study area for the entire NDREB time series (December 2018 to June 2023) (Reynolds et al., 2008). A GAM was employed to examine the potential effect of temperature on the seasonal area time series using the mgcv package (Pedersen et al., 2019; Wood, 2017). Since the seasonal time series was dependent on image availability and is therefore not continuous, we generated a 7-day average temperature prior to each kelp forest area measurement. We conducted the GAM analysis with a smoothing parameter (k) of 60 for *in situ* temperature and 100 for satellite SST. Following the smoothing, we examined the k-index, which indicated values very near to or exceeding 1 in both cases. The regression basis used for each variable was "cr" (cubic regression), the family was Gaussian and the method "REML". Both GAM models were parsed using Akaike Information Criteria (AIC) to determine which temperature model (*in situ* or satellite) best fits the *M. pyrifera* area data (Burnham and Anderson, 2002).

Water samples were collected at the same locations in the kelp bed to determine nutrient concentrations (nitrite, nitrate, silicate, phosphate), following a standard protocol Rev 03/2019 GG/KS, at approximately monthly intervals from December 2021 to March 2023. We used the average nutrients value of the three sites considering that our satellite-based approach allowed for the examination of the entire kelp forest area. We also calculated the N:P ratio by summing nitrite and nitrate, and subsequently dividing by phosphate. Given the small size of the dataset, we used a linear model for nutrient analysis. Prior to this, a visual inspection of the data indicated very high values for some nutrients. Consequently, we conducted linear regressions independently to assess the potential impact of each nutrient on the population area. For a more comprehensive understanding of nutrient dynamics in the Punta de Parra population, we analyzed our *in situ* nutrient data alongside data from an offshore station (36° 30.80'S, 73° 7.75'W) (Farías et al., 2021) using Pearson correlation analysis.

Data on significant wave height (Hs) and maximum wave height (Hmax) were obtained from the Hydrographic and Oceanographic Service of the Chilean Navy (SHOA) and used to examine their potential effect on the kelp forest area estimates and dynamics. Data was available from October 24, 2017, to March 8, 2021, collected at Talcahuano, a port located astride Concepcion bay from our study site. As the seasonal time series is dependent on image availability and not continuous, we calculated a 7-day average for Hs and Hmax on the days leading up to each kelp forest area measurement. We used a GAM analysis using the mgcv package, with a smoothing parameter (k) of 60, a cubic regression basis (cr), a Gaussian family, and the REML method (Pedersen et al., 2019). Only Hs yielded a significant result, so the analysis was repeated using this variable alone with the same parameters.

Significant height of combined wind waves and swell (SWH), Free convective velocity over the oceans (CV) (m s^{-1}), surface net solar radiation (SSR)(J m^{-2}), total precipitation (TP)(m), and U-component (eastward) of wind (u10)(m s^{-1}) were downloaded from ERA5 reanalysis for the period (December 2018 to June 2023) (Hersbach et al., 2020). This period was chosen to synchronize with the S2 time series developed. The ERA5 reanalysis, created by the European Center for Medium-Range Weather Forecasts (ECMWF), presents an extensive global archive of atmospheric, land surface, and ocean wave conditions since 1950 (Hersbach et al., 2020). Notably, it features an enhanced spatial resolution of 0.25° and delivers hourly output.

For the statistical analysis, we first plotted the environmental variables alongside the time series of *M. pyrifera* area to visually assess potential relationships. Given the seasonal nature of the time series, a linear correlation between the dependent variable (area) and the independent variables (environmental drivers) was not evident, in light of this, a GAM was chosen for the analysis. A monthly average of all variables and the area were computed prior to analysis (Wood, 2017). The GAM analysis was conducted with a smoothing parameter (k) of 40 for each variable. Subsequently, the k-index was examined, revealing values very close to or greater than 1 in all cases. The basis used for each variable was "cr" (cubic regression). To account for the seasonal variability in our analysis, we included a cyclic cubic spline term for the month variable with k=10. The family was Gaussian and the method "REML". The analysis was conducted in R Studio using the mgcv package (Pedersen et al., 2019). From this initial analysis, only solar radiation exhibited a significance value of less than 0.05 (R-sq.(adj) = 0.584, Deviance explained = 77.8%). Subsequently, a second GAM analysis was conducted, focusing solely on solar radiation and its relationship with the area of the kelp forest.

2.5. Biomass estimation

Biomass estimation sampling was conducted in the Punta de Parra population during summer of 2023, employing the methodology detailed in McPherson and Kudela (2022). Over three days, spaced one month apart, data collection took place at the same three specified sited where were we obtained temperature and nutrient *in situ* data. A total of 18 *M. pyrifera* canopies of different individuals were weighed on the boat using a portable scale. Depth measurements were taken before collecting the individuals for weighing. Onshore, we counted the number of blades, fronds, and measured the longest frond for each individual. We then used linear regression to examine the association between biomass (kg) and the number of blades and fronds. To estimate kelp density, we conducted a total of 8 transects (20 × 1 m) across the three study sites, which correspond to the buoy locations where *in situ* temperature was measured. In each transect, all individuals within the area were counted. On the other hand, we computed the NDREB index using S2 images corresponding to the days of the transect surveys following the previously described method. Subsequently, we applied linear regression models to analyze kelp density, using the counts from the 8 transects as an approximation of density and the NDREB values obtained of four pixels at the transect location. All statistical analyses were performed using RStudio version 2023.9.1.494 (R Core Team, 2022).

3. Results

3.1. Long term annual canopy series with Landsat dataset

The annual time series yielded 23 years of data (1999–2022) for the *M. pyrifera* forest area at Punta de Parra (Fig. 3). No discernible positive or negative trend was identified for the series. The maximum area recorded was 2.484 ha in 2021, while the minimum area was observed in 2020, measuring 0.351 ha. A strong positive correlation was observed between kelp forest area between satellites sensors, reaching 0.96 between L5 and L7, and 0.90 between L7 and L8. The time series, derived from annual compilations, displayed notable variability with a distinct pattern of fluctuating area over time. It is noteworthy that the extensive L7 series consistently exhibits no area less than 1 ha, except for 2020, which saw a significant decrease. Regarding the statistical analysis, none of the ENSO indices was significantly associated with the annual time series. However, a notable difference was observed in the variance explained by the ENSO indices with no lag (Adjusted R^2 = −0.0999, deviance explained = 5.01%), which increased when a 1-year lag was applied (Adjusted R^2 = 0.138, deviance explained = 31.3%).

3.2. Seasonal canopy series with Sentinel 2

The seasonal time series derived using NDREB with the dynamic threshold revealed a seasonal pattern, with peak area values during austral summer and troughs in winter (Fig. 4). The maximal area recorded reached 3.571 ha during the austral summer of 2021, while the minimum was observed in austral winter 2019, with an area of only 0.047 ha. Similar to the annual series, the notable decrease in area observed during the 2020 period stands out. Furthermore, the seasonal time series created with the conservative threshold (> 0) revealed a similar seasonal pattern 4. The maximum value was found in the summer of 2023, reaching 3.887 ha. The latter value is closely followed by the outlier detected in summer 2020 (3.756 ha), during which no values above 1 ha were observed for the entire season. The minimal value recorded in the time series was 0.013 ha during the winter of 2019, consistent with the values observed in the series using dynamic thresholds. The correlation between the time series using dynamic thresholds and the conservative approach was strongly positive (r = 0.84). Turbidity, assessed via the NDTI index, showed a seasonal pattern with peak values during summer, reaching a maximum of −0.03, signifying heightened turbidity during these months. Conversely, the lowest values were recorded in winter, with a minimum of −0.98, indicative of greater water column clarity during this period (see Fig. 4). Regarding the effect of turbidity and sea level on the visualization of the *M. pyrifera* population at Punta de Parra, we detected variations between conservative and dynamic thresholds (Table 1). Overall, the joint effect of turbidity and sea level explained more variability in the data with the conservative threshold (R^2 = 0.18), than with the dynamic threshold (R^2 = 0.14). Hence, we used the time series with the dynamic threshold to test the effects of different environmental variables on the satellite canopy area. Seasonally, we observed a greater effect in winter (R^2 = 0.38). When examined separately, tidal height had similar effects between thresholds (R^2 = 0.12, Supplementary Table 7). However, we noted differences in the impact of turbidity on satellite canopy area (R^2 = 0.05 and 0.11, see Supplementary Table 8). The correlation between turbidity and sea level was weakly negative (−0.28).

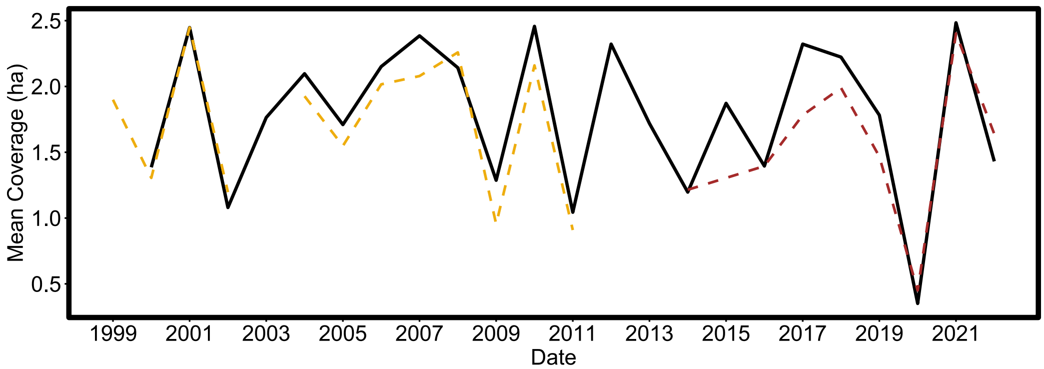

Fig. 3. Time series of *M. pyrifera* population area at Punta de Parra extracted from Landsat imagery (1999–2022). In yellow with dashed line Landsat 5 satellite images, in black Landsat 7 images and in red with dashed lines Landsat 8 images. (For interpretation of the references to color in this figure legend, the reader is referred to the web version of this article.)

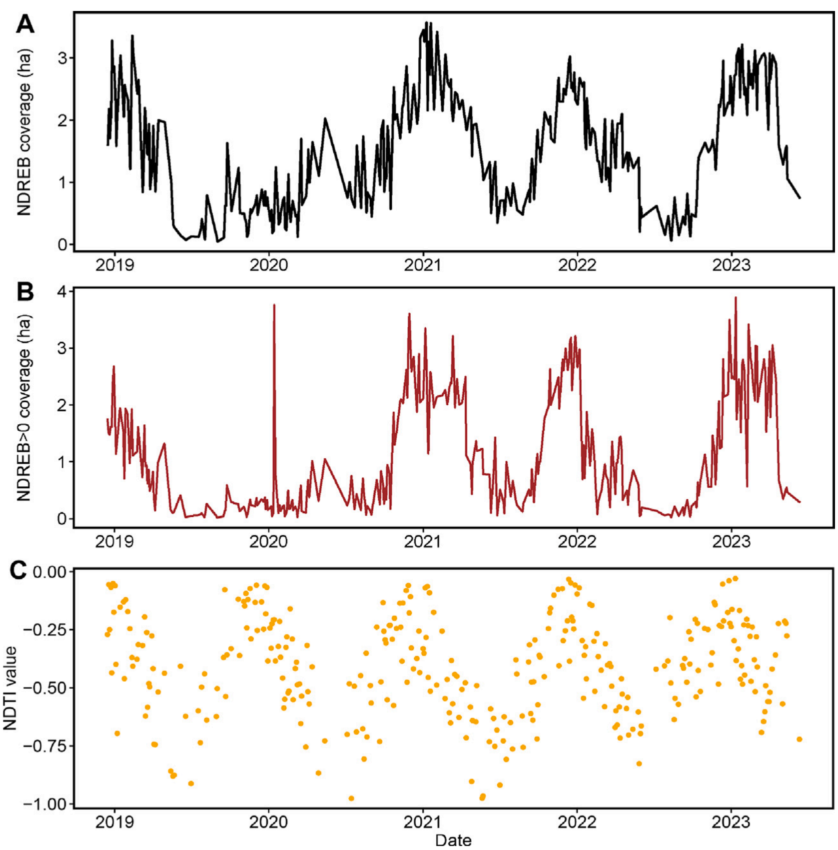

Fig. 4. Seasonal time series of the *Macrocystis pyrifera* population area at Punta de Parra, derived from Sentinel-2 imagery (2019–2023). (A) NDREB vegetation index time series using a dynamic threshold. (B) NDREB vegetation index time series using a conservative threshold (values > 0). (C) NDTI turbidity index time series.

The *in situ* temperature fluctuated between of 17.02 °C in January 2022 (summer) and a minimum value of 9.99 °C in October 2022 (spring), with greater variability during the spring and summer months (Fig. 5A). This variable showed a significant effect on the area of the *M. pyrifera* forest (Table 2). In comparison, satellite SST also showed significant effect, but explained deviance less variance. The SST time series exhibited a clear seasonal pattern, with the highest values occurring in summer and the lowest in winter (Fig. 8).

When comparing the models, the AIC of the GAMs indicated that the *in situ* temperature model provided a better fit (AIC = 211.88) compared to the satellite SST GAM (AIC = 810.71). Notably, the correlation between *in situ* temperature and satellite-derived SST was weak (Pearson's r = 0.332, R^2 = 0.11). Additionally, a systematic bias was observed, with satellite measurements consistently overestimating temperatures compared to *in situ* measurements (Bias = −4.33).

Significant wave height also influenced kelp forest area, though the deviance explained was low (6.98%). A seasonal pattern was evident, with larger wave heights during winter months (Fig. 8). Among the environmental variables derived from ERA5, only solar radiation (SSR) showed a significant statistical relationship with the kelp forest area (Table 2). The SSR time series followed a distinct seasonal pattern, peaking in summer and reaching its lowest values in winter (Fig. 8). Notably, SSR data were unavailable during winter months due to cloud cover, resulting in missing values for that period.

Regarding nutrients, elevated levels of nitrate and silicate were observed during the autumn and winter months, whereas nitrite and phosphate levels remained relatively constant throughout the year (Fig.

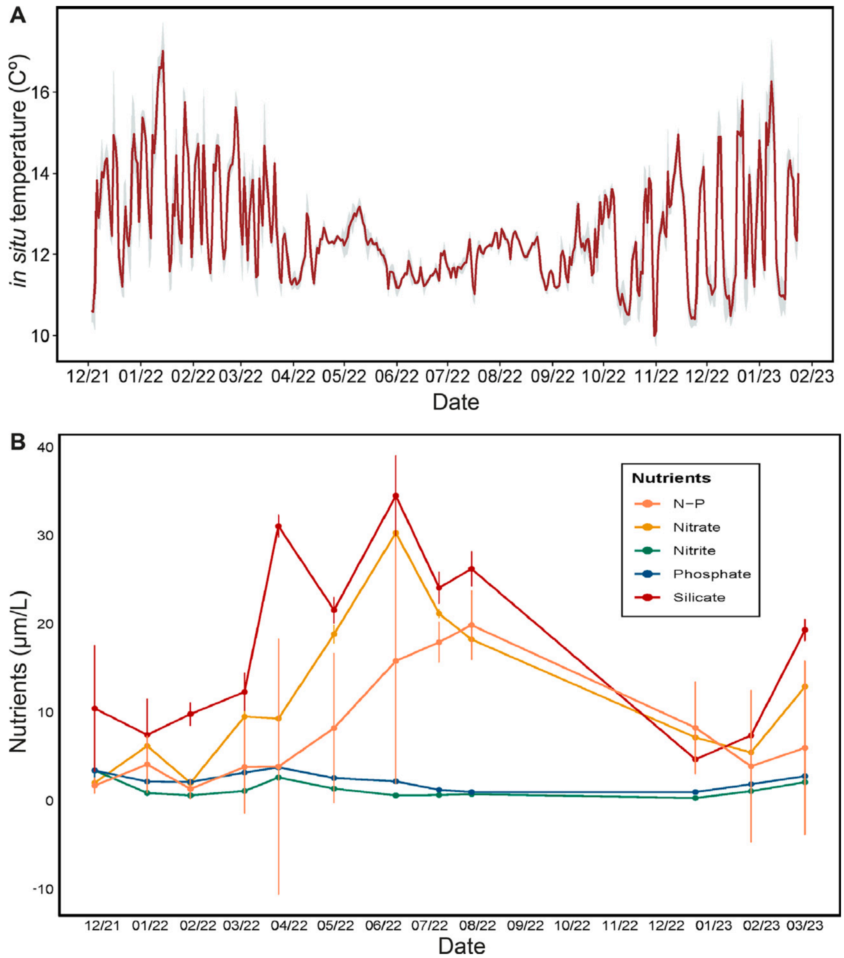

Fig. 5. (A) Time series of *in situ* temperature data at Punta de Parra. The red line is the daily average, while the gray shading indicates the daily standard deviation. (B) Time series of *in situ* nutrient values at Punta de Parra. (For interpretation of the references to color in this figure legend, the reader is referred to the web version of this article.)

Table 1
Results of multiple linear regression analysis for *Macrocystis pyrifera* canopy area in Punta de Parra using the NDREB index (Normalized Difference Red-Edge/Blue Index) as the response variable. Predictor variables include the NDTI index (Normalized Difference Turbidity Index) and tidal height. Results are presented for each season and for the entire time series (December 2018 to June 2023). The table includes values for both thresholds (dynamic and conservative), showing the adjusted coefficient of determination (R^2 Adj) and the number of satellite images (n) used in the analysis.

Season	Threshold	R^2 (Adj)	n
Summer	dynamic	0.06	119
Autumn	dynamic	0.15	66
Winter	dynamic	0.38	52
Spring	dynamic	0.06	83
Total	dynamic	0.14	320
Summer	conservative	0.12	119
Autumn	conservative	0.1	66
Winter	conservative	0.33	52
Spring	conservative	0.09	83
Total	conservative	0.18	320

5B). Among these, nitrate, silicate, and the N:P ratio were found to have significant effects on the area of *M. pyrifera* (Table 3). Offshore nutrient data, in contrast, exhibited a different seasonal pattern, with high nitrate values during the summer (Fig. 7). However, no significant correlations were found between *in situ* and offshore nutrient concentrations (Fig. 10).

3.3. Biomass estimation

We found a robust positive relationship between the number of blades and biomass (kg), which was weaker when comparing the number of fronds and biomass (kg) (Table 4, Fig. 6). Extrapolating these relationships to satellite-derived canopy area revealed a positive and significant relationship between density transects and NDREB values (Table 4, Fig. 9). The relationship between kelp density and NDREB values was weak (R^2= 0.18), likely influenced by the limited number of transects (n = 8) conducted during the austral summer of 2023. Therefore, we focused on analyzing kelp forest area time series.

4. Discussion

4.1. Long term annual canopy series with Landsat dataset

Kelp forests ecosystems have provided vital resources for generations of inhabitants of the southeastern Pacific shores (Aguilera et al., 2019; Alcalde et al., 2023). The growing pressures of harvesting and climate change highlight the need to understand their dynamics for better management. Along the coast of Chile, most attention on giant kelp forests has been focused on extraction in the northern sector or the climatic refugia on the southern extreme, leaving central Chile understudied. The 24-year time series of a *M. pyrifera* forest in Central Chile is a unique contribution to understand kelp dynamics of the vast central region. The annual time series exhibited the high variability observed in other giant kelp populations, characterized by fluctuating

Table 2
Results of the generalized additive models (GAMs) examining the relationship between the seasonal time series of *Macrocystis pyrifera* canopy area and environmental drivers. The table reports the estimated degrees of freedom (EDF), F-statistic, *p*-value, adjusted coefficient of determination (R^2 Adj), and the percentage of deviance explained for each environmental variable: *in situ* temperature, satellite-derived sea surface temperature (SST), significant wave height, and solar radiation.

Environmental drivers	Edf	F-Statistic	*p*-value	R^2 (Adj)	Deviance explained
in situ temperature	3.36	3.96	0.004	0.17	19.6%
SST satellite	3.17	13.91	<0.001	0.15	15.6%
Significant wave height	1.05	11.57	<0.001	0.06	6.98%
Solar radiation	12.82	2.19	0.038	0.38	57.9%

Table 3
Results of the linear regression analysis examining the relationship between the seasonal time series of *Macrocystis pyrifera* canopy area and *in situ* nutrient concentrations (nitrate, nitrite, silicate, and phosphate). The table presents the F-statistic, *p*-value, and adjusted coefficient of determination (R^2 Adj) for each nutrient variable.

Variable	F-Statistic	*p*-value	R^2 (Adj)
Nitrate	15.97	0.003	0.565
Nitrite	0.56	0.47	−0.041
Phosphate	0.42	0.533	−0.056
N:P	17.25	0.002	0.5963
Silicate	22.71	<0.001	0.664

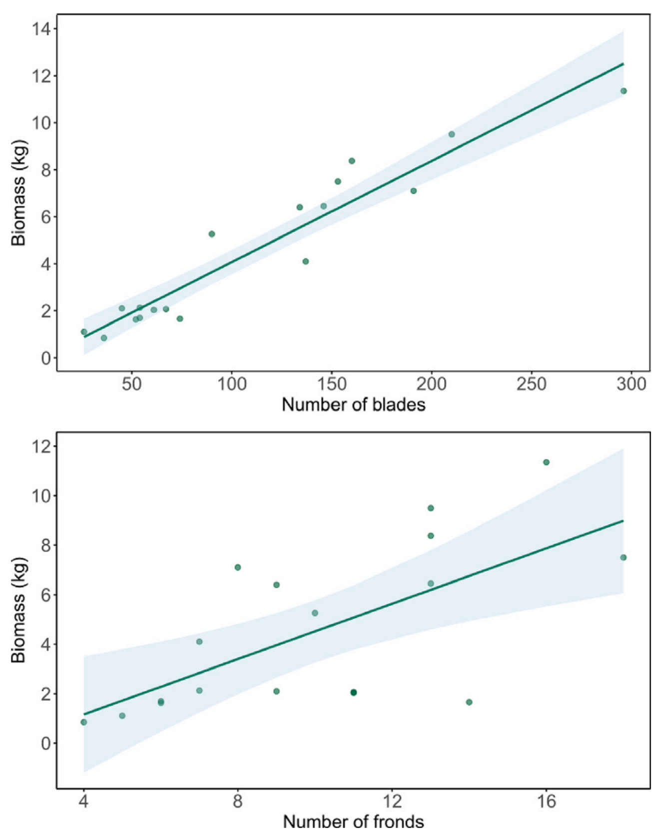

Fig. 6. Kelp canopy biomass (kg) scatter plot against number of blades (upper) and fronds (down) with the regression line for Punta de Parra.

area from year to year with no discernible trends (Cavanaugh et al., 2011; Friedlander et al., 2020; Bell et al., 2023).

A number of studies in populations of *M. pyrifera* along the coast of southern Australia, Chile and California have shown that the growth of subtidal stands are strongly seasonal and depend on the supply of nutrients by different oceanographic processes, together with low–frequency, large–scale climatic disturbances such as ENSO cycles (Dayton et al., 1999; Reed et al., 2011). In contrast to findings in other studies (Butler et al., 2020; Bell et al., 2020; Friedlander et al., 2020) but consistent with findings from the Falkland-Malvinas Islands (Houskeeper et al., 2022), our analysis did not reveal a significant association with ENSO variability on the same year. Nonetheless, the variance explained increased when introducing a 1-year lag, similar to locations around the Southern ocean (Tierra del Fuego and Falkland-Malvinas, Friedlander et al., 2020; Houskeeper et al., 2022), which suggests delayed effects of ENSO events on giant kelp populations (Pfister et al., 2018). The seasonal upwelling in central Chile is correlated to the annual migration of the South Pacific Subtropical Anticyclone (Ancapichún and Garcés-Vargas, 2015). ENSO events modify seasonal upwelling in central Chile — delayed during El Niño and advanced during La Niña — which has important implications for SST and nutrient supply (Muñoz et al., 2023). Also, the absence of a discernible trend in kelp forest area suggests that recent changes in Conception Bay's regime, driven by increased upwelling pulses even during winter, or alterations in precipitation patterns, may not have had a significant influence on kelp biomass dynamics (Schneider et al., 2017; Bustos-Espinoza et al., 2024). To clarify the phenological effects of seasonal upwelling on central Chile's giant kelp forests will require long-term time series with validation over temporal scales that can capture the seasonal cycle in biomass dynamics. A potential approach to reliably capture seasonal and phenological patterns using remote sensing estimates involves multiple validations per year over multiple years, an approach that has proven effective in capturing multispecies dynamics (Bell et al., 2020; Lønborg et al., 2021; Cingano et al., 2024).

4.2. *Seasonal variability in the canopy series with Sentinel 2*

Although the annual kelp forest area time series offers valuable insights, the strong seasonal population dynamics generates strong variability during the year, which was the rationale for generating a high temporal resolution series. The monthly area fluctuations over four and a half years exhibited a clear seasonal pattern characterized by summer peaks and winter troughs, aligning with patterns described for other population in central Chile (Buschmann et al., 2004; Almanza and Buschmann, 2013). Increases during spring-summer correlated with higher radiation values and the period of more intense upwelling documented for Concepción Bay (Sobarzo et al., 2007). The pattern aligns with the analysis of environmental variables, where we identified an influence of temperature, nitrate, silicate, and solar radiation on the dynamics of the Punta de Parra kelp forest area.

Notably, both the annual and seasonal time series showed a decrease in area in 2020. None of the environmental variables analyzed exhibited anomalous values for that year, we lack empirical data to explain that occurred during the summer of 2020. Moreover, the pronounced variation in area we report between 2020 and 2021 fits with the exceptional growth rates of *M. pyrifera*, which can exceed 30 cm per day under favorable conditions (Van Tussenbroek, 1989; Graham et al., 2007). This rapid growth enables *M. pyrifera* forests to recover from seasonal disturbances and quickly expand their canopy. On the other hand, seasonal stressors such as reduced solar radiation, increased wave activity, and nutrient fluctuations during winter months can cause massive biomass reductions (Dayton et al., 1992; Reed et al., 2015b). Our findings underscore the strong influence of environmental drivers on kelp forest dynamics, with summer conditions promoting dense, expansive canopies and winter conditions leading to significant canopy

Table 4
Result of the linear regression analysis for estimating the biomass (kg) of *Macrocystis pyrifera* using the number of canopy blades and the number of canopy fronds as predictor variables. Additionally, the results of the linear regression analysis between the density transect and NDREB values are shown. The table includes the slope, intercept, adjusted coefficient of determination (R^2 Adj), F-statistic, and the number of observations (n).

Giant kelp	Slope	Intercept	R^2 (Adj)	F-Statistic	n
Number of canopy blades Biomass (kg)	0.04 ± 0.003	−0.23 ± 0.43	0.91	170.3	18
Number of canopy fronds Biomass (kg)	0.56 ± 0.16	−1.07 ± 1.66	0.45	12.93	18
Density transect NDREB values	41.28 ± 14.96	21.886 ± 6.26	0.18	7.61	8

reductions. Seasonal variability was well represented in our field observations in Punta de Parra; summer surveys revealed thick, multilayered fronds that hindered diving, while winter surveys show a noticeably sparser surface presence. While previous studies may have underestimated these dynamics due to the limited temporal resolution of field observations (Schiel and Foster, 2015), our use of high-frequency satellite imagery offers a more comprehensive perspective, highlighting the critical role of remote sensing in capturing the dynamic nature of kelp forests.

The Punta de Parra population, situated near the coast, may experience various factors that could potentially influence its satellite visualization, such as sand from the beach, rocky substrate, or wave activity (Bell et al., 2020). Therefore, we opted for the finest spatial resolution of S2 images, along with a dynamic threshold and the NDREB index. A reduced effect of turbidity was noted when employing the dynamic threshold developed by Cavanaugh et al. (2021b). The creation of a unique threshold for each scene enables the classification of kelp pixels according to changing conditions throughout the year, rendering it suitable for generating a seasonal time series. Additionally, the utilization of the NDREB index facilitated enhanced visualization of the kelp, attributed to its incorporation of the Red-edge band (see 4), which has demonstrated superior effectiveness in detecting submerged kelp (Timmer, 2022; Timmer et al., 2024). This index is useful for coastal regions, where waves and tides often make it challenging to observe the canopy.

Colored dissolved organic matter (CDOM), suspended solids (SS), turbidity, and other compounds such as silica, phosphate, nitrite, or nitrate are common in aquatic environments (Paudel et al., 2016; Curra-Sánchez et al., 2022, 2024; García-Tuñon et al., 2024). Among these, turbidity is a critical indicator for assessing aquatic ecosystem health. Remote sensing offers a robust tool for long-term turbidity monitoring, utilizing diverse algorithms, indices, and band ratios (Elhag et al., 2019; Lizcano-Sandoval et al., 2022; García-Tuñon et al., 2024; Jiang et al., 2024; Zhang et al., 2024). For instance, García-Tuñon et al. (2024) applied S2 imagery to generate a turbidity time series in northern Chilean Patagonia, highlighting influences from precipitation, river discharge, and wind. Similarly, Elhag et al. (2019) and Zhang et al. (2024) used the Normalized Difference Turbidity Index (NDTI) with S2 imagery to achieve reliable turbidity estimates in a dam and a lake, respectively. Lizcano-Sandoval et al. (2022) employed NDTI to map temporal changes in submerged seagrass in west-central Florida. However, this study represents the first application of NDTI to monitor kelp forests, highlighting its potential for macroalgal ecosystems. Our findings reveal that NDTI's performance in our study area was highly sensitive to seasonal fluctuations (see Fig. 4), likely driven by coastal biophysical variability, including wind-driven upwelling, runoff and frequent algal blooms (Mahmoud et al., 2023).

Temperature plays a crucial role on *M. pyrifera* life cycle at the local scale (Schiel and Foster, 2015; Hollarsmith et al., 2020). The impact of temperature on giant kelp forests has been thoroughly investigated, particularly in recent studies focusing on its relationship with heatwaves (Cavanaugh et al., 2019; Tait et al., 2021). In contrast to other regions worldwide, central Chile has been experiencing a trend of decreasing coastal temperatures in recent decades (Marin et al., 2021). On the other hand, no demonstrable effect on *Macrocystis* populations in Patagonia has been observed from marine heatwave or marine cold-spells highlighting this region as a possible climatic refugium (Mora-Soto et al., 2022). Impacts can vary by region, as local adaptations of populations to different temperatures have been demonstrated (Hollarsmith et al., 2020). Specifically in central Chile, models predicting an increase in the intensity of summer upwelling, coupled with observations of more frequent upwelling-favorable wind pulses during winter, could mitigate the impact of high temperatures on populations in this region (Echevin et al., 2012; Bustos-Espinoza et al., 2024). A recent observation indicated a favorable performance of *M. pyrifera* juvenile sporophytes from central Chile across different temperatures, albeit with the potential risk of reduction at 16 °C (Solas et al., 2024). In our study in central Chile, we did not observe *in situ* temperature values beyond the recognized range for *Macrocystis* between 4 and 20 °C (Schiel and Foster, 2015). Therefore, we found no evidence of thermal stress at the population of Punta de Parra. Although the time series for *in situ* temperature was much shorter compared to the satellite SST (1 year vs. 4 years), it yielded better results in the statistical analysis underscoring the importance of *in situ* variables in kelp forests. The overestimation of satellite SST values compared to *in situ* temperature values is expected because the latter are continuous and include nighttime measurements. This, combined with the low resolution of the satellite data and effects of the coastal systems like tidal mixing, may be contributing to the low correlation between the two temperature series.

A strong inverse correlation between temperature and nitrate concentration in the water column, particularly in upwelling ecosystems, is well-documented (Nielsen and Navarrete, 2004; Palacios et al., 2013; Farías et al., 2021). In our study area, the Bay of Concepción, upwelling shows a seasonal component with a predominance in spring and summer, and an intensification of upwelling has been reported over the past few decades (Sobarzo et al., 2007; Schneider et al., 2017; Farías et al., 2021). Nutrients in CB have been observed to follow the same seasonal pattern, with high values in spring and summer, leading to increased productivity as measured by chlorophyll-a, which also peaks in summer (Farias et al., 1996; Morales et al., 2007; Bustos-Espinoza et al., 2024). In contrast, measurements taken within the kelp population of Punta de Parra revealed a different pattern, with maximum values occurring during autumn–winter season (Fig. 5). Supporting this, we also found no correlation between the *in situ* nutrients and the offshore nutrients. This disparity suggest that the metabolic activity of the kelp plays a more significant role in influencing local seawater dynamics compared to temperature/nutrients changes driven by seasonal upwelling (Murie and Bourdeau, 2020). It can be concluded that the low nitrate levels during spring and summer at Punta de Parra are a result of nutrient uptake by the *Macrocystis* population, when the kelp canopy area is at its peak. The high nitrate and silicate values observed during winter coincide with the period when the smallest satellite-detected kelp area is recorded. Due to a hibernation-like period where nutrient utilization decreases, coupled with and increase in upwelling pulses during the winter season, we hypothesize that these factors lead to higher nutrient concentrations in the water column during this time within the *M. pyrifera* forest (Bustos-Espinoza et al., 2024).

Among nutrients, nitrate has received increased attention in explaining the dynamics of *Macrocystis* forests (Zimmerman and Kremer, 1986; Rodriguez et al., 2016). Giant kelp growth becomes nutrient-limited below approximately 1 μM nitrate (Graham et al., 2007). In this regard, our study reveals that we did not encounter any nitrate values below this threshold (Fig. 5), indicating no evidence that this could limit the forest growth. It has been observed that *Macrocystis* forests utilize less than 5% of the nitrate that reaches them, with the remainder obtained from other sources, such as ammonium from epibionts (Fram et al., 2008). This emphasizes the importance of collecting nutrient data within the forest itself, as in the present study. In forests of the nearby Falkland-Malvinas region, nitrate content — estimated from temperature-nitrate relationships — was a primary driver of canopy area observed using Landsat imagery (Houskeeper et al., 2022), but *in situ* sampling to confirm the efficacy of the nitrogen estimations was unavailable.

Wave disturbance is one of the most important variable in kelp forest dynamics (Graham et al., 2007; Elsmore et al., 2024). Concepcion Bay is exposed to the ocean from the north, where prevailing winds from May to July intensify wave action (Sobarzo et al., 1997; Muñoz et al., 2023). This period coincides with the lowest observed kelp area in the population and high wave heights. Given the statistical significance, we conclude that wave action partly explains the seasonality of the population.

Among the other environmental variables examined, only solar radiation was significantly associated to kelp forest dynamics. Radiation is recognized as a growth-limiting factor for *M. pyrifera*, with high radiance in shallow waters (Graham, 1996), and low radiance particularly in high latitudes (Palacios et al., 2021). In Punta de Parra, the highest summer solar radiance coincided with the greatest satellite coverage of the forest. Higher productivity in *Macrocystis* has been linked to increased irradiance, which also boosts its photoprotection and antioxidant capacity (Celis-Plá et al., 2021). Another factor to consider is that the highest turbidity was also observed in summer, making it difficult for light to penetrate the water column. Poor water clarity is synergistic with other stressors, such as temperature, causing a greater loss of area in *Macrocystis* forests (Tait et al., 2021). While precipitation was not significantly associated to kelp forest dynamics, changes in salinity have been identified as a modulating factor for spore release (Buschmann et al., 2004). In other populations, spore release predominantly occurred during winter months when salinity decreased due to precipitation input, both directly and through river channels (Buschmann et al., 2004). Given the changing precipitation regime over recent decades, alterations in oceanographic dynamics within the BC are becoming apparent (Bustos-Espinoza et al., 2024). For future studies, may investigate temporal changes in spore abundance and examine its relation with satellite-based phenological data.

While our study provides valuable insights into the seasonal and interannual dynamics of *M. pyrifera* in Punta de Parra, several limitations warrant consideration. The relatively short duration of *in situ* environmental measurements, particularly for temperature and nutrient data, limited our ability to capture long-term trends and their potential impacts on kelp forest dynamics. Additionally, discrepancies between *in situ* measurements and satellite-derived data, such as temperature, highlight the challenges of accurately characterizing coastal systems influenced by complex processes like tidal mixing and nocturnal cooling (Susanto et al., 2018; Kachelein et al., 2024). Our study focused on a single population, which limits the generalization of our findings to regions with differing environmental and ecological conditions. Furthermore, while satellite-based indices have proven invaluable for monitoring kelp forests, they are vulnerable to interference from factors such as turbidity, sand, and other factors can result in over- or underestimations of kelp canopy area (Cavanaugh et al., 2021a). For example, tidal fluctuations can significantly affect the detection of kelp canopies by altering water levels and the visibility of the canopy at the surface, thereby introducing potential inaccuracies in area estimation (Timmer et al., 2024). Although we identified significant correlations between kelp cover and environmental variables, establishing causality remains challenging due to the observational nature of the study. Future research should focus on integrating longer *in situ* time series, increasing spatial replication across multiple populations, and employing experimental approaches to better understand the physiological responses of *M. pyrifera* to changing environmental conditions. Such efforts would provide deeper insights into the complex interactions driving kelp forest dynamics and enhance the robustness of predictions for their future trajectories under climate change. Recognizing these limitations is essential for interpreting our findings and highlights the need for continued research that combines remote sensing and *in situ* methodologies to achieve a more holistic understanding of kelp forest ecosystems.

The observation of seasonal patterns holds promise for furnishing critical insights into the prudent management and sustainable exploitation of these kelp forests in Chile (Carranza et al., 2024). Continuous monitoring of giant kelp populations is crucial for identifying significant changes, including those driven by contemporary climate change, essential for developing effective conservation strategies (Beas-Luna et al., 2020). In this regard, Chile, Peru, and Argentina lags significantly behind in collecting information on kelp forests. However, recent improvements in the automation of kelp classification for Landsat observations (Finger et al., 2021; Houskeeper et al., 2022) has resulted in the recent addition of multi-decadal time series for forests of the Falkland-Malvinas islands, Peru, and Argentina regions to the open-access Kelpwatch repository (Bell et al., 2023). With the additional pressure of intense extraction in Chile and Peru due to high demand from China, the stage is set for overexploitation and the potential disappearance of kelp forests in the Southeast Pacific (Kang et al., 2023). In the future, expanding the generation of seasonal time series for several populations of *M. pyrifera* across Chile will yield valuable insights, not only regarding stressors but also for implementing harvesting closures.

4.3. Biomass estimation

The limited dataset obtained in the field may not suffice to establish a meaningful correlation between the observed biomass and the satellite data. Nonetheless, the *in situ* is crucial for guiding future research initiatives (McPherson and Kudela, 2022). The *in situ* relationship between biomass and frond/stipe counts holds significant value for future surveys and provides a reference point for the seasonal populations of central Chile. Our results align with allometric data from other populations. The strongest relationship for estimating biomass was with the number of blades (R^2 = 0.91, slope = 0.04), similar to those found in California by McPherson and Kudela (2022) (R^2 = 0.81, slope = 0.03). Based on these results, and considering that blades contribute the most to sporophyte weight, we suggest using the number of blades as the primary metric for estimating *M. pyrifera* biomass (Reed et al., 2015a). In terms of the frond count for biomass estimation, the R^2 value was lower, mirroring results found in northern, central, and southern California (Rassweiler et al., 2018; Santa Barbara Coastal et al., 2021; McPherson and Kudela, 2022). Another recent study conducted in Chilean Patagonia reported frond counts and wet biomass in *M. pyrifera* the coefficient of determination values for frond number were higher than in our study, and even higher when compared to California (Santa Barbara Coastal et al., 2021; McPherson and Kudela, 2022; Palacios et al., 2024). Although counting blades can provide better results, it is more labor-intensive and time-consuming compared to counting fronds, making it potentially less practical in remote locations.

Given the weak relationship between kelp density and NDREB values (R^2= 0.18), we did not attempt to reconstruct a biomass time series using this index. Instead, we focused on kelp forest area as a more reliable proxy for canopy dynamics. This decision was based on the limited number of transects available and the relatively high variability observed in the regression analysis, which suggested that NDREB alone may not be a strong predictor of biomass at the scale of our study. In the future, there is a need to augment and sustain monitoring efforts to facilitate the creation of biomass estimates. However, replicating monitoring programs like the one undertaken in California with the Santa Barbara Coastal Long Term Ecological Research project may not always be viable for other countries. In the case of Chile, with its vast coastline and challenging accessibility, implementing a similar program would pose considerable challenges.

5. Conclusion

The kelp *Macrocystis pyrifera* play a crucial role as habitat-forming species worldwide. In Chile is key component of coastal socio-ecological systems and remote sensing can provide substantial help for kelp monitoring along its extensive and rugged coastal terrain. By integrating satellite observations spanning decades and seasons with limited but intensive field data, we have advanced the understanding of the dynamics of a central Chilean *M. pyrifera* population. The pronounced seasonality, with peak coverage in summer and minimal in winter, aligned closely with variations in temperature, wave height and solar radiation. Notably, we found no *in situ* evidence of temperature or nutrient stress limiting *M. pyrifera* growth. It can be concluded that the primary factors driving the seasonality in our study site were solar radiation and wave action.

Further field data collection is essential to establish robust correspondence between *in situ* observations and satellite-derived data, particularly for accurate biomass estimation. Our findings underscore the importance of understanding the seasonal dynamics and the environmental drivers influencing different underwater forests. Moving forward, efforts to integrate and validate remote sensing data with on-the-ground observations will be critical to enhance our ability to monitor, manage and conserve kelp ecosystems.

CRediT authorship contribution statement

Daniel Gonzalez-Aragon: Writing – review & editing, Writing – original draft, Visualization, Validation, Supervision, Software, Resources, Project administration, Methodology, Investigation, Funding acquisition, Formal analysis, Data curation, Conceptualization. **Richard Muñoz:** Writing – review & editing, Writing – original draft, Validation, Methodology, Formal analysis, Data curation. **Henry Houskeeper:** Writing – review & editing, Writing – original draft, Validation, Methodology, Formal analysis, Data curation, Conceptualization. **Kyle Cavanaugh:** Writing – review & editing, Supervision, Software, Methodology, Conceptualization. **Wirmer García-Tuñon:** Writing – review & editing, Writing – original draft, Validation, Methodology, Investigation. **Laura Farías:** Writing – review & editing, Data curation. **Carlos Lara:** Writing – review & editing, Supervision, Funding acquisition, Conceptualization. **Bernardo R. Broitman:** Writing – review & editing, Writing – original draft, Validation, Supervision, Investigation, Funding acquisition, Conceptualization.

Declaration of Generative AI and AI-assisted technologies in the writing process

During the preparation of this work, the author(s) used ChatGPT to refine the writing. After using this tool/service, the author(s) reviewed and edited the content as needed and take (s) full responsibility for the content of the publication.

Declaration of competing interest

The authors declare the following financial interests/personal relationships which may be considered as potential competing interests: Daniel Gonzalez-Aragon reports financial support was provided by Catholic University of the Holy Conception - San Andrés Campus. Daniel Gonzalez-Aragon reports a relationship with Catholic University of the Holy Conception - San Andrés Campus that includes: funding grants. If there are other authors, they declare that they have no known competing financial interests or personal relationships that could have appeared to influence the work reported in this paper.

Acknowledgments

We extend our gratitude to the Hydrographic and Oceanographic Service of the Chilean Navy (SHOA) for providing the Talcahuano tide data. BRB acknowledges support from FONDECYT 1221699, 1221534 and the Instituto Milenio SECOS (CN2019_015). C.L. acknowledge funding by FONDECYT 1230420.

Appendix A. Supplementary data

Supplementary material related to this article can be found online at https://doi.org/10.1016/j.ecoinf.2025.103103.

Data availability

Following the guidelines of Huettmann and Arhonditsis (2023), our Google Earth Engine (GEE) code is available at https://code.earthengine.google.com/df92ced1763815d2d520dc23ab0b5814. The raw data generated in this study are openly available on Zenodo: https://doi.org/10.5281/zenodo.14975329.

References

Aguilera, M.A., Aburto, J.A., Bravo, L., Broitman, B.R., García, R.A., Gaymer, C.F., Gelcich, S., López, B.A., Montecino, V., Pauchard, A., et al., 2019. Chile: environmental status and future perspectives. In: World Seas: An Environmental Evaluation. Elsevier, pp. 673–702.

Alcalde, V., Flores, C., Guardia, J., Olguín, L., Broitman, B.R., 2023. Marine invertebrates as proxies for early kelp use along the western coast of South America. Front. Earth Sci. 11.

Almanza, V., Buschmann, A.H., 2013. The ecological importance of Macrocystis pyrifera (Phaeophyta) forests towards a sustainable management and exploitation of Chilean coastal benthic co-management areas. Int. J. Environ. Sustain. Dev. 12 (4), 341–360.

Ancapichún, S., Garcés-Vargas, J., 2015. Variability of the Southeast Pacific Subtropical Anticyclone and its impact on sea surface temperature off north-central Chile. Cienc. Mar. 41 (1), 1–20.

Assis, J., Alberto, F., Macaya, E.C., Castilho Coelho, N., Faugeron, S., Pearson, G.A., Ladah, L., Reed, D.C., Raimondi, P., Mansilla, A., et al., 2023. Past climate-driven range shifts structuring intraspecific biodiversity levels of the giant kelp (Macrocystis pyrifera) at global scales. Sci. Rep. 13 (1), 12046.

Beas-Luna, R., Micheli, F., Woodson, C.B., Carr, M., Malone, D., Torre, J., Boch, C., Caselle, J.E., Edwards, M., Freiwald, J., et al., 2020. Geographic variation in responses of kelp forest communities of the California current to recent climatic changes. Global Change Biol. 26 (11), 6457–6473.

Bell, T.W., Allen, J.G., Cavanaugh, K.C., Siegel, D.A., 2020. Three decades of variability in California's giant kelp forests from the Landsat satellites. Remote Sens. Environ. 238, 110811.

Bell, T.W., Cavanaugh, K.C., Reed, D.C., Siegel, D.A., 2015a. Geographical variability in the controls of giant kelp biomass dynamics. J. Biogeogr. 42 (10), 2010–2021.

Bell, T.W., Cavanaugh, K.C., Saccomanno, V.R., Cavanaugh, K.C., Houskeeper, H.F., Eddy, N., Schuetzenmeister, F., Rindlaub, N., Gleason, M., 2023. Kelpwatch: A new visualization and analysis tool to explore kelp canopy dynamics reveals variable response to and recovery from marine heatwaves. PLoS One 18 (3), e0271477.

Bell, T.W., Cavanaugh, K.C., Siegel, D.A., 2015b. Remote monitoring of giant kelp biomass and physiological condition: An evaluation of the potential for the Hyperspectral Infrared Imager (HyspIRI) mission. Remote Sens. Environ. 167, 218–228.

Bennion, M., Fisher, J., Yesson, C., Brodie, J., 2019. Remote sensing of kelp (Laminariales, Ochrophyta): monitoring tools and implications for wild harvesting. Rev. Fish. Sci. Aquac. 27 (2), 127–141.

Betancourtt, C., Zapata, J., Latorre, N., Anguita, C., Castañeda, F., Meynard, A., Fierro, C., Espinoza, C., Guajardo, E., Núñez, A., et al., 2018. Variación espacio-temporal en la composición del ensamble de macroalgas del intermareal rocoso de Maitencillo, Valparaíso, costa central de Chile. Rev. de Biología Mar. Y Oceanografía 53 (1), 105–117.

Borchers, H.W., 2023. pracma: Practical numerical math functions. CRAN, R package version 2.4.4.

Burnham, K.P., Anderson, D.R., 2002. Model Selection and Multimodel Inference: A Practical Information-Theoretic Approach. Springer.

Buschmann, A.H., Moreno, C., Vásquez, J.A., Hernández-González, M.C., 2006. Reproduction strategies of Macrocystis pyrifera (Phaeophyta) in Southern Chile: the importance of population dynamics. J. Appl. Phycol. 18, 575–582.

Buschmann, A.H., Prescott, S., Potin, P., Faugeron, S., Vasquez, J.A., Camus, C., Infante, J., Hernández-González, M.C., Gutierrez, A., Varela, D.A., 2014. The status of kelp exploitation and marine agronomy, with emphasis on Macrocystis pyrifera, in Chile. In: Advances in Botanical Research, vol. 71, Elsevier, pp. 161–188.

Buschmann, A.H., Vásquez, J.A., Osorio, P., Reyes, E., Filún, L., Hernández-González, M.C., Vega, A., 2004. The effect of water movement, temperature and salinity on abundance and reproductive patterns of *Macrocystis* spp. (Phaeophyta) at different latitudes in Chile. Mar. Biol. 145, 849–862.

Bustos-Espinoza, L., Torres-Ramírez, P., Figueroa, S., González, P.S., Pavez, M.A., Jerez, R., Saldías, G.S., Espinoza, C., Galán, A., 2024. Biogeochemical response of the water column of Concepción Bay, Chile, to a new regime of atmospheric and oceanographic variability. Geosciences 14 (5), 125.

Butler, C.L., Lucieer, V.L., Wotherspoon, S.J., Johnson, C.R., 2020. Multi-decadal decline in cover of giant kelp Macrocystis pyrifera at the southern limit of its Australian range. Mar. Ecol. Prog. Ser. 653, 1–18.

Carranza, D.M., Wieters, E.A., Vásquez, J.A., Stotz, W.B., 2024. Exploring the consequences of kelp removal: a review shows we are missing a broader perspective. Biodivers. Conserv. 1–37.

Cavanaugh, K.C., Bell, T., Costa, M., Eddy, N.E., Gendall, L., Gleason, M.G., Hessing-Lewis, M., Martone, R., McPherson, M., Pontier, O., et al., 2021a. A review of the opportunities and challenges for using remote sensing for management of surface-canopy forming kelps. Front. Mar. Sci. 1536.

Cavanaugh, K.C., Cavanaugh, K.C., Bell, T.W., Hockridge, E.G., 2021b. An automated method for mapping giant kelp canopy dynamics from UAV. Front. Environ. Sci. 8, 587354.

Cavanaugh, K.C., Reed, D.C., Bell, T.W., Castorani, M.C., Beas-Luna, R., 2019. Spatial variability in the resistance and resilience of giant kelp in southern and Baja California to a multiyear heatwave. Front. Mar. Sci. 6, 413.

Cavanaugh, K.C., Siegel, D.A., Kinlan, B.P., Reed, D.C., 2010. Scaling giant kelp field measurements to regional scales using satellite observations. Mar. Ecol. Prog. Ser. 403, 13–27.

Cavanaugh, K.C., Siegel, D.A., Reed, D.C., Dennison, P.E., 2011. Environmental controls of giant-kelp biomass in the Santa Barbara Channel, California. Mar. Ecol. Prog. Ser. 429, 1–17.

Celis-Plá, P.S., Kappes, J.L., Figueroa, F.L., Pereda, S.V., Villegas, K., Altamirano, R., Hernández-González, M.C., Buschmann, A.H., 2021. Solar radiation as an isolated environmental factor in an experimental mesocosm approach for studying photosynthetic acclimation of Macrocystis pyrifera (Ochrophyta). Front. Plant Sci. 12, 622150.

Cingano, P., Vuerich, M., Petruzzellis, F., Orzan, L., Trotta, G., Casolo, V., Asquini, E., Bacaro, G., Boscutti, F., 2024. Seagrasses on the move: Tracing the multi-decadal species distribution trends in lagoon meadows using Landsat imagery. Ecol. Informatics 82, 102685.

Claverie, M., Ju, J., Masek, J.G., Dungan, J.L., Vermote, E.F., Roger, J.-C., Skakun, S.V., Justice, C., 2018. The Harmonized Landsat and Sentinel-2 surface reflectance data set. Remote Sens. Environ. 219, 145–161.

Colombo-Pallotta, M.F., García-Mendoza, E., Ladah, L.B., 2006. Photosynthetic performance, light absorption, and pigment composition of Macrocystis pyrifera (laminariales, phaeophyceae) blades from different depths 1. J. Phycol. 42 (6), 1225–1234.

Cuba, D., Guardia-Luzon, K., Cevallos, B., Ramos-Larico, S., Neira, E., Pons, A., Avila-Peltroche, J., 2022. Ecosystem services provided by kelp forests of the humboldt current system: A comprehensive review. Coasts 2 (4), 259–277.

Curra-Sánchez, E.D., Lara, C., Cornejo-D'Ottone, M., Nimptsch, J., Aguayo, M., Broitman, B.R., Saldías, G.S., Vargas, C.A., 2022. Contrasting land-uses in two small river basins impact the colored dissolved organic matter concentration and carbonate system along a river-coastal ocean continuum. Sci. Total Environ. 806, 150435.

Curra-Sánchez, E.D., Valerio, A.d.M., Lara, C., García-Tuñon, W., Broitman, B.R., Saldías, G.S., Nimptsch, J., Vargas, C.A., 2024. CDOM dynamics in two coastal zones influenced by contrasting land uses in northern patagonia. Estuar. Coast. Shelf Sci. 306, 108897.

Dayton, P.K., Tegner, M.J., Edwards, P.B., Riser, K.L., 1999. Temporal and spatial scales of kelp demography: The role of oceanographic climate. Ecol. Monograph. 69, 219–250.

Dayton, P.K., Tegner, M.J., Parnell, P.E., Edwards, P.B., 1992. Temporal and spatial patterns of disturbance and recovery in a kelp forest community. Ecol. Monograph. 62 (3), 421–445.

Duarte, C.M., Gattuso, J.P., Hancke, K., Gundersen, H., Filbee-Dexter, K., Pedersen, M.F., Middelburg, J.J., Burrows, M.T., Krumhansl, K.A., Wernberg, T., Moore, P., Pessarrodona, A., Ørberg, S.B., Pinto, I.S., Assis, J., Queirós, A.M., Smale, D.A., Bekkby, T., Serrão, E.A., Krause-Jensen, D., 2022. Global estimates of the extent and production of macroalgal forests. Glob. Ecol. Biogeogr. 31, 1422–1439.

Echevin, V., Goubanova, K., Belmadani, A., Dewitte, B., 2012. Sensitivity of the Humboldt Current system to global warming: a downscaling experiment of the IPSL-CM4 model. Clim. Dyn. 38, 761–774.

Eger, A.M., Marzinelli, E.M., Beas-Luna, R., Blain, C.O., Blamey, L.K., Byrnes, J.E., Carnell, P.E., Choi, C.G., Hessing-Lewis, M., Kim, K.Y., et al., 2023. The value of ecosystem services in global marine kelp forests. Nat. Commun. 14 (1), 1894.

Elhag, M., Gitas, I., Othman, A., Bahrawi, J., Gikas, P., 2019. Assessment of water quality parameters using temporal remote sensing spectral reflectance in arid environments, Saudi Arabia. Water 11 (3), 556.

Elsmore, K., Nickols, K.J., Miller, L.P., Ford, T., Denny, M.W., Gaylord, B., 2024. Wave damping by giant kelp, Macrocystis pyrifera. Ann. Botany 133 (1), 29–40.

ESA, 2015. Sentinel-2 user handbook, tools, and exploitation. ESA Stand. Doc. Date 1, 1–64.

Faraw, J.J., 2015. Practical Regression and ANOVA Using R.

Farias, L., Chuecas, L.A., Salamanca, M.A., 1996. Effect of coastal upwelling on nitrogen regeneration from sediments and ammonium supply to the water column in Concepcion Bay, Chile. Estuar. Coast. Shelf Sci. 43 (2), 137–155.

Farías, L., Manríquez, V., Maza, L.d.l., 2021. Más de 20 años de monitoreo del sistema de surgencia costera de Chile central. Universidad de Concepción.

Fell, F., 2022. A contrast minimization approach to remove sun glint in Landsat 8 imagery. Remote. Sens. 14 (18), 4643.

Finger, D.J., McPherson, M.L., Houskeeper, H.F., Kudela, R.M., 2021. Mapping bull kelp canopy in northern California using Landsat to enable long-term monitoring. Remote Sens. Environ. 254, 112243.

Flanders Marine Institute (VLIZ); Intergovernmental Oceanographic Commission (IOC), 2023. Sea level station monitoring facility. https://www.ioc-sealevelmonitoring.org. (Accessed on 30 May 2023 at VLIZ).

Fornes, A., Basterretxea, G., Orfila, A., Jordi, A., Álvarez, A., Tintoré, J., 2006. Mapping *Posidonia oceanica* from IKONOS. ISPRS J. Photogramm. Remote Sens. 60 (5), 315–322.

Fram, J.P., Stewart, H.L., Brzezinski, M.A., Gaylord, B., Reed, D.C., Williams, S.L., MacIntyre, S., 2008. Physical pathways and utilization of nitrate supply to the giant kelp, Macrocystis pyrifera. Limnol. Oceanogr. 53 (4), 1589–1603.

Frangoudes, K., et al., 2011. Seaweeds fisheries management in France, Japan, Chile and Norway. CBM- Cah. de Biologie Mar. 52 (4), 517.

Friedlander, A.M., Ballesteros, E., Bell, T.W., Caselle, J.E., Campagna, C., Goodell, W., Hüne, M., Muñoz, A., Salinas-de León, P., Sala, E., et al., 2020. Kelp forests at the end of the earth: 45 years later. PLoS One 15 (3), e0229259.

Friedlander, A.M., Ballesteros, E., Bell, T.W., Giddens, J., Henning, B., Hüne, M., Muñoz, A., Salinas-de León, P., Sala, E., 2018. Marine biodiversity at the end of the world: Cape Horn and Diego Ramírez islands. PLoS One 13 (1), e0189930.

García-Tuñon, W., Curra-Sánchez, E.D., Lara, C., González-Rodríguez, L., Urrego, E.P., Delegido, J., Broitman, B.R., 2024. Spatio-temporal variability of turbidity derived from Sentinel-2 in Reloncavísound, Northern Patagonia, Chile. Ecol. Informatics 83, 102814.

Gonzalez-Aragon, D., Rivadeneira, M.M., Lara, C., Torres, F.I., Vásquez, J.A., Broitman, B.R., 2024. A species distribution model of the giant kelp Macrocystis pyrifera: worldwide changes and a focus on the southeast Pacific. Ecol. Evol. 14 (3), e10901.

Gorelick, N., Hancher, M., Dixon, M., Ilyushchenko, S., Thau, D., Moore, R., 2017. Google earth engine: Planetary-scale geospatial analysis for everyone. Remote Sens. Environ. 202, 18–27.

Graham, M.H., 1996. Effect of high irradiance on recruitment of the giant kelp Macrocystis (phaeophyta) in shallow water 1. J. Phycol. 32 (6), 903–906.

Graham, M.H., Vasquez, J.A., Buschmann, A.H., et al., 2007. Global ecology of the giant kelp Macrocystis: from ecotypes to ecosystems. Ocean. Mar. Biology 45, 39.

Hamilton, S.L., Bell, T.W., Watson, J.R., Grorud-Colvert, K.A., Menge, B.A., 2020. Remote sensing: generation of long-term kelp bed data sets for evaluation of impacts of climatic variation. Ecology 101 (7), e03031.

Hersbach, H., Bell, B., Berrisford, P., Hirahara, S., Horányi, A., Muñoz-Sabater, J., Nicolas, J., Peubey, C., Radu, R., Schepers, D., et al., 2020. The ERA5 global reanalysis. Q. J. R. Meteorol. Soc. 146 (730), 1999–2049.

Hollarsmith, J.A., Buschmann, A.H., Camus, C., Grosholz, E.D., 2020. Varying reproductive success under ocean warming and acidification across giant kelp (Macrocystis pyrifera) populations. J. Exp. Mar. Biology Ecol. 522, 151247.

Houskeeper, H.F., Rosenthal, I.S., Cavanaugh, K.C., Pawlak, C., Trouille, L., Byrnes, J.E., Bell, T.W., Cavanaugh, K.C., 2022. Automated satellite remote sensing of giant kelp at the Falkland Islands (Islas Malvinas). PLoS One 17 (1), e0257933.

Huettmann, F., Arhonditsis, G., 2023. Towards an ecological informatics scholarship that is reflective, repeatable, transparent, and sharable!. Ecol. Informatics 76, 102132.

Huovinen, P., Ramírez, J., Palacios, M., Gómez, I., 2020. Satellite-derived mapping of kelp distribution and water optics in the glacier impacted Yendegaia Fjord (Beagle Channel, Southern Chilean Patagonia). Sci. Total Environ. 703, 135531.

Jiang, J., Chen, Z., Sun, K., Chen, Y., Mu, M., Sun, Q., Zeng, S., 2024. Monitoring 36-year water clarity dynamics in turbid waters of the Pearl River Estuary, China, using Landsat data. Ecol. Informatics 81, 102600.

Kachelein, L., Gille, S.T., Mazloff, M.R., Cornuelle, B.D., 2024. Characterizing non-phase-locked tidal currents in the California current system using high-frequency radar. J. Geophys. Research: Ocean. 129 (7), e2023JC020340.

Kang, H., Yang, Z., Zhang, Z., 2023. The competitiveness of China's seaweed products in the international market from 2002 to 2017. Aquac. Fish. 8 (5), 579–586.

Kopczak, C.D., Zimmerman, R.C., Kremer, J.N., 1991. Variation in nitrogen physiology and growth among geographically isolated populations of the giant kelp, Macrocystis pyrifera (phaeophyta) 1. J. Phycol. 27 (2), 149–158.

Krausman, P.R., Cain, J.W., 2022. Wildlife Management and Conservation: Contemporary Principles and Practices. JHU Press.

Li, J., Wang, L., Liu, S., Peng, B., Ye, H., 2022. An automatic cloud detection model for Sentinel-2 imagery based on Google Earth Engine. Remote. Sens. Lett. 13 (2), 196–206.
Lizcano-Sandoval, L., Anastasiou, C., Montes, E., Raulerson, G., Sherwood, E., Muller-Karger, F.E., 2022. Seagrass distribution, areal cover, and changes (1990–2021) in coastal waters off West-Central Florida, USA. Estuar. Coast. Shelf Sci. 279, 108134.
Lønborg, C., Thomasberger, A., Stæhr, P.A., Stockmarr, A., Sengupta, S., Rasmussen, M.L., Nielsen, L.T., Hansen, L.B., Timmermann, K., 2021. Submerged aquatic vegetation: Overview of monitoring techniques used for the identification and determination of spatial distribution in European coastal waters. Integr. Environ. Assess. Manag. 18 (4), 892–908.
Mace, G.M., Reynolds, J.D., 2001. Exploitation as a conservation issue. Conserv. Exploit. Species 6, 1.
Mahmoud, S.H., Ahmed, S.S., Zhu, D.Z., Gan, T.Y., Loewen, M.R., van Duin, B., Mahmood, K., 2023. Monitoring the spatial distribution of water quality of an urban stormwater pond using satellite images. Ecol. Informatics 77, 102205.
Marin, M., Bindoff, N.L., Feng, M., Phillips, H.E., 2021. Slower long-term coastal warming drives dampened trends in coastal marine heatwave exposure. J. Geophys. Research: Ocean. 126 (11), e2021JC017930.
McPherson, M.L., Kudela, R.M., 2022. Kelp patch-specific characteristics limit detection capability of rapid survey method for determining canopy biomass using an unmanned aerial vehicle. Front. Environ. Sci. 10, 690963.
Mora-Soto, A., Aguirre, C., Iriarte, J., Palacios, M., Macaya, E., Macias-Fauria, M., 2022. A song of wind and ice: Increased frequency of marine cold-spells in Southwestern Patagonia and their possible effects on giant Kelp forests. J. Geophys. Research: Ocean. 127 (6), e2021JC017801.
Mora-Soto, A., Capsey, A., Friedlander, A.M., Palacios, M., Brewin, P.E., Golding, N., Dayton, P., Van Tussenbroek, B., Montiel, A., Goodell, W., et al., 2021. One of the least disturbed marine coastal ecosystems on earth: Spatial and temporal persistence of Darwin's sub-Antarctic giant kelp forests. J. Biogeogr. 48 (10), 2562–2577.
Mora-Soto, A., Palacios, M., Macaya, E.C., Gómez, I., Huovinen, P., Pérez-Matus, A., Young, M., Golding, N., Toro, M., Yaqub, M., et al., 2020. A high-resolution global map of giant kelp (Macrocystis pyrifera) forests and intertidal green algae (ulvophyceae) with Sentinel-2 imagery. Remote. Sens. 12 (4), 694.
Morales, C.E., González, H.E., Hormazabal, S.E., Yuras, G., Letelier, J., Castro, L.R., 2007. The distribution of chlorophyll-a and dominant planktonic components in the coastal transition zone off Concepción, central Chile, during different oceanographic conditions. Prog. Oceanogr. 75 (3), 452–469.
Muñoz, R., Vergara, O.A., Figueroa, P.A., Mardones, P., Sobarzo, M., Saldías, G.S., 2023. On the phenology of coastal upwelling off central-southern Chile. Dyn. Atmos. Oceans 104, 101405.
Murie, K.A., Bourdeau, P.E., 2020. Fragmented kelp forest canopies retain their ability to alter local seawater chemistry. Sci. Rep. 10 (1), 11939.
National Oceanic and Atmospheric Administration, 2023. Nino 3.4 index. http://psl.noaa.gov/gcos_wgsp/Timeseries/Nino34/index.html. (Accessed: 16 July 2023).
Nielsen, K.J., Navarrete, S.A., 2004. Mesoscale regulation comes from the bottom-up: intertidal interactions between consumers and upwelling. Ecol. Lett. 7 (1), 31–41.
Nijland, W., Reshitnyk, L., Rubidge, E., 2019. Satellite remote sensing of canopy-forming kelp on a complex coastline: a novel procedure using the Landsat image archive. Remote Sens. Environ. 220, 41–50.
Palacios, D.M., Hazen, E.L., Schroeder, I.D., Bograd, S.J., 2013. Modeling the temperature-nitrate relationship in the coastal upwelling domain of the California current. J. Geophys. Research: Ocean. 118 (7), 3223–3239.
Palacios, M., Osman, D., Ramírez, J., Huovinen, P., Gómez, I., 2021. Photobiology of the giant kelp Macrocystis pyrifera in the land-terminating glacier fjord Yendegaia (Tierra del Fuego): A look into the future? Sci. Total Environ. 751, 141810.
Palacios, M.A., Pessarrodona, A., Huovinen, P., Gomez, I., Mora-Soto, A., 2024. First estimates of standing crop and net primary production from giant Kelp forests in Southern Patagonia during the Austral summer. SSRN, Available at SSRN: https://ssrn.com/abstract=4783884 or http://dx.doi.org/10.2139/ssrn.4783884,
Paudel, B., Velinsky, D., Belton, T., Pang, H., 2016. Spatial variability of estuarine environmental drivers and response by phytoplankton: A multivariate modeling approach. Ecol. Informatics 34, 1–12.
Pedersen, E.J., Miller, D.L., Simpson, G.L., Ross, N., 2019. Hierarchical generalized additive models in ecology: an introduction with mgcv. PeerJ 7, e6876.
Pérez-Cutillas, P., Pérez-Navarro, A., Conesa-García, C., Zema, D.A., Amado-Álvarez, J.P., 2023. What is going on within google earth engine? A systematic review and meta-analysis. Remote. Sens. Applications: Soc. Environ. 29, 100907.
Pessarrodona, A., Assis, J., Filbee-Dexter, K., Burrows, M.T., Gattuso, J.-P., Duarte, C.M., Krause-Jensen, D., Moore, P.J., Smale, D.A., Wernberg, T., 2022. Global seaweed productivity. Sci. Adv. 8, 2465.
Pfister, C.A., Berry, H.D., Mumford, T., 2018. The dynamics of Kelp Forests in the Northeast Pacific ocean and the relationship with environmental drivers. J. Ecol. 106 (4), 1520–1533.
QGIS Development Team, 2022. QGIS geographic information system. Open Source Geospatial Foundation.
R Core Team, 2022. R: A language and environment for statistical computing. R Foundation for Statistical Computing, Vienna, Austria.
Ramón, A.B., Anny, R.G., Victorino, M.M., 1983. Circulation and fertility of waters in Concepcion Bay. Estuar. Coast. Shelf Sci. 16 (1), 95–105.
Rassweiler, A., Reed, D.C., Harrer, S.L., Nelson, J.C., 2018. Improved estimates of net primary production, growth, and standing crop of Macrocystis pyrifera in Southern California. Ecology 99 (9).
Reed, D.C., Brzezinski, M.A., 2009. Kelp forests. Manag. Nat. Coast. Carbon Sink. 31.
Reed, D.C., Carlson, C.A., Halewood, E.R., Nelson, J.C., Harrer, S.L., Rassweiler, A., Miller, R.J., 2015a. Patterns and controls of reef-scale production of dissolved organic carbon by giant kelp M acrocystis pyrifera. Limnol. Oceanogr. 60 (6), 1996–2008.
Reed, D.C., Rassweiler, A., Carr, M.H., Cavanaugh, K.C., Malone, D.P., Siegel, D.A., 2011. Wave disturbance overwhelms top-down and bottom-up control of primary production in California kelp forests. Ecology 92, 2108–2116.
Reed, D.C., Rassweiler, A.R., Miller, R.J., Page, H.M., Holbrook, S.J., 2015b. The value of a broad temporal and spatial perspective in understanding dynamics of kelp forest ecosystems. Mar. Freshwater Res. 67 (1), 14–24.
Reynolds, R.W., Banzon, V.F., NOAA CDR Program, 2008. NOAA Optimum Interpolation 1/4 Degree Daily Sea Surface Temperature (OISST) Analysis, Version 2. http://dx.doi.org/10.7289/V5SQ8XB5, SST. NOAA National Centers for Environmental Information. [15/10/2023].
Rodriguez, G.E., Reed, D.C., Holbrook, S.J., 2016. Blade life span, structural investment, and nutrient allocation in giant kelp. Oecologia 182, 397–404.
Rudolph, A., Franco, C., Becerra, J., Barros, A., Ahumada, R., 2002. Evaluación de materia orgánica e hidrocarburos aromáticos policíclicos en sedimentos superficiales, bahía Concepción-Chile. Boletin de la Soc. Chil. de Qu´ i Mica 47 (4), 403–410.
Saavedra, N., 1980. La presión y la dirección del viento en Concepción. Tralka 1 (2), 153–162.
Santa Barbara Coastal, L., Bell, T.W., Cavanaugh, K.C., Reuman, D., Castorani, M.C., Sheppard, L., Walter, J., 2021. SBC LTER: REEF: Macrocystis pyrifera biomass and environmental drivers in southern and central California. NSF Public Access Repository (NSF-PAR).
Schiel, D.R., Foster, M.S., 2015. The Biology and Ecology of Giant Kelp Forests. Univ of California Press.
Schneider, W., Donoso, D., Garcés-Vargas, J., Escribano, R., 2017. Water-column cooling and sea surface salinity increase in the upwelling region off central-south Chile driven by a poleward displacement of the South Pacific high. Prog. Oceanogr. 151, 38–48.
Sedgwick, P., 2012. Pearson's correlation coefficient. Bmj 345.
SERNAPESCA, 2021. Anuarios Estadísticos De Pesca Y Acuicultura. Subsecretaría de Pesca y Acuicultura, Ministerio de Economía Fomento y Reconstrucción, Gobierno de Chile.
Setyawidati, N., Kaimuddin, A., Wati, I., Helmi, M., Widowati, I., Rossi, N., Liabot, P., Stiger-Pouvreau, V., 2018. Percentage cover, biomass, distribution, and potential habitat mapping of natural macroalgae, based on high-resolution satellite data and in situ monitoring, at Libukang Island, Malasoro Bay, Indonesia. J. Appl. Phycol. 30 (1), 159–171.
Silva, J., Zemelman, R., Mandoca, M.A., Henríquez, M., Merino, C., González, C., 1987. Antibiotic-resistant gram negative bacilli isolated from sea water and shellfish: possible epidemiological implications. Rev. Latinoam. Microbiol 165–169.
Sobarzo, M., Bravo, L., Donoso, D., Garcés-Vargas, J., Schneider, W., 2007. Coastal upwelling and seasonal cycles that influence the water column over the continental shelf off central Chile. Prog. Oceanogr. 75 (3), 363–382.
Sobarzo, M., Figueroa, D., Arcos, D., 1997. The influence of winds and tides in the formation of circulation layers in a Bay, a case study: Concepción Bay, Chile. Estuar. Coast. Shelf Sci. 45 (6), 729–736.
Solas, M., Correa, R.A., Barría, F., Garcés, C., Camus, C., Faugeron, S., 2024. Assessment of local adaptation and outbreeding risks in contrasting thermal environments of the giant kelp, Macrocystis pyrifera. J. Appl. Phycol. 36 (1), 471–483.
Steneck, R.S., Graham, M.H., Bourque, B.J., Corbett, D., Erlandson, J.M., Estes, J.A., Tegner, M.J., 2002. Kelp forest ecosystems: biodiversity, stability, resilience and future. Environ. Conserv. 29 (4), 436–459.
Stewart, H., Fram, J., Reed, D., Williams, S., Brzezinski, M., Macintyre, S., Gaylord, B., 2009. Differences in growth, morphology and tissue carbon and nitrogen of Macrocystis pyrifera within and at the outer edge of a giant kelp forest in California, USA. Mar. Ecol. Prog. Ser. 375, 101–112.
Susanto, R.D., Pan, J., Devlin, A.T., 2018. Tidal mixing signatures in the Hong Kong coastal waters from satellite-derived sea surface temperature. Remote. Sens. 11 (1), 5.
Tait, L.W., Thoral, F., Pinkerton, M.H., Thomsen, M.S., Schiel, D.R., 2021. Loss of giant kelp, Macrocystis pyrifera, driven by marine heatwaves and exacerbated by poor water clarity in New Zealand. Front. Mar. Sci. 8, 721087.
Timmer, B., 2022. The Effects of Kelp Canopy Submersion on the Remote Sensing of Surface-Canopy Forming Kelps (Ph.D. thesis). University of Victoria.
Timmer, B., Reshitnyk, L.Y., Hessing-Lewis, M., Juanes, F., Gendall, L., Costa, M., 2024. Capturing accurate kelp canopy extent: integrating tides, currents, and species-level morphology in kelp remote sensing. Front. Environ. Sci. 12, 1338483.
Van Tussenbroek, B., 1989. Observations on branched Macrocystis pyrifera (L.) C. Agardh (Laminariales, Phaeophyta) in the Falkland Islands. Phycologia 28 (2), 169–180.
Vásquez, J.A., 2016. The brown seaweeds fishery in Chile. In: Fisheries and Aquaculture in the Modern World. INTECH, pp. 123–141.

Vásquez, J.A., Morales, C., Vallone, A., 2024. Brown seaweeds fishery and copper mining production: Two distant economic industries connected by socioecological impacts in Northern Chile. Mar. Policy 165, 106191.

Wood, S.N., 2017. Generalized Additive Models: An Introduction with R. Chapman and Hall/CRC.

Xu, H., 2006. Modification of Normalised Difference Water Index (NDWI) to enhance open water features in remotely sensed imagery. Int. J. Remote Sens. 27 (14), 3025–3033.

Zhang, J., Meng, F., Fu, P., Jing, T., Xu, J., Yang, X., 2024. Tracking changes in chlorophyll-a concentration and turbidity in Nansi Lake using Sentinel-2 imagery: A novel machine learning approach. Ecol. Informatics 81, 102597.

Zimmerman, R.C., Kremer, J.N., 1986. In situ growth and chemical composition of the giant kelp, Macrocystis pyrifera: response to temporal changes in ambient nutrient availability. Mar. Ecol. Prog. Ser. 27 (2), 277–285.